

Inverse Quadratic Decay in Random Subset Sum

Edwin Chen

Dept. of Electrical and Computer Engineering, Portland
State University
Portland, OR, USA
echen1ffa@gmail.com

Christof Teuscher

Dept. of Electrical and Computer Engineering, Portland
State University
Portland, OR, USA
teuscher@pdx.edu

Abstract

The Subset Sum Problem is a fundamental NP-complete problem in cryptography and combinatorial optimization, with many real-world applications. The Random Subset Sum Problem (RSSP) is a more applicable version of subset sum, where numbers are drawn from some i.i.d input distribution. We present an algorithm that, with probability $1 - \delta$, constructs the same $O(B/w)$ mesh as Da Cunha et al. [Da Cunha et al. 2023], while trimming to w elements throughout and running in $O(w \log w)$ time. Then, we present a novel beam search heuristic running in linearithmic time w.r.t list size n and beam width w using the mesh that gives an expected error of $O\left(\frac{B}{nw^2}\right)$ under a standard mean-field assumption with equal standard deviation, demonstrating the practical effectiveness of meshing to achieve error decay. The algorithm is empirically robust to multiple input distributions and can naturally extend to variants with simple changes to the scoring heuristic, establishing a new practical baseline for robust subset sum error decay and ϵ -approximation theory.

CCS Concepts

• **Theory of computation** \rightarrow **Approximation algorithms analysis**; • **Mathematics of computing** \rightarrow *Probability and statistics*.

Keywords

Subset Sum, Beam Search, Random Instances, Error Decay, Heuristics, Meet-in-the-Middle

1 Introduction

The Subset Sum problem is a classic NP-complete problem [Garey and Johnson 1979] with applications in resource allocation [Abboud et al. 2019], cryptography [Bonnetain et al. 2020], financial auditing [Biesner et al. 2022], and combinatorial optimization. Given a multiset $S \subseteq \mathbb{Z}$ and a target $T \in \mathbb{Z}$, the goal is to find a subset $V \subseteq S$ whose sum is as close as possible to T :

$$\text{Answer}(S, T) = \min_{V \subseteq S} \left| \sum_{v \in V} v - T \right|. \quad (1)$$

We study the Random Subset Sum Problem (RSSP), where n i.i.d. weights are drawn from a fixed distribution, typically $U(1, B)$, focusing on expected error decay for RSSP, which is useful well beyond cryptographic settings.

We present and evaluate a simple beam search heuristic and prove:

- **Explicit-Constant meshing bound:** Phase A fills all w buckets with probability at least $1 - \delta$ in $7.96 \log_2 w + 5.19 \log_2(1/\delta) + O(1)$ iterations, implying an $O(B/w)$ mesh constructed in $O(w \log w)$ time with width- w trimming at every step.

- **MITM beam:** $\mathbb{E}[\text{error}] = O(B/(nw^2))$ with asymptotically equal standard deviation.
- **Complexity:** $O(nw \log w)$ time and $O(w)$ memory for search; exact reconstruction in $O(nw)$ time with $O(w\sqrt{n})$ memory.
- **Robustness:** The guarantees hold, up to constants, for a broad class of i.i.d. input distributions; empirical results match the theory.

To our knowledge, prior work has not emphasized expected error-decay rates for RSSP; many papers focus on uniform inputs (Sections 2.3, 2.4) or worst-case settings (Section 2.1). For the methods that have a similar scope to our heuristic (Section 2.2), our analysis and experiments suggest the proposed heuristic is a practical baseline for robust Subset Sum approximation.

2 Related Works

2.1 Exact and Approximate Algorithms for the Deterministic Version

When all elements of S are nonnegative, both exact and approximation schemes are well studied. The classic dynamic program runs in pseudo-polynomial time $\tilde{O}(nw_{\max})$, where $w_{\max} = \max S$. Chen et al. [Chen et al. 2024b] improved this to $O(n + w_{\max}^{3/2})$. Fully Polynomial-Time Approximation Schemes (FPTAS) such as Gens and Levner [Gens and Levner 1979] and Chen et al. [Chen et al. 2024a] offer guarantees with near-optimal dependence on ϵ , the relative error. Table 1 summarizes representative results we compare against.

2.2 Heuristic Methods

Heuristics are attractive for large or mixed-sign instances where exact or FPTAS methods can be slow or inapplicable. Representative approaches include Genetic Algorithms [Goldberg 1989; Nguyen and Caldas 2004], Simulated Annealing [Kirkpatrick et al. 1983], Particle Swarm Optimization (PSO) [Kennedy and Eberhart 1995], Tabu Search [Glover 1986, 1989, 1990], and the Arithmetic Optimization Algorithm (AOA) [Madugula et al. 2022]. Table 2 summarizes typical characteristics.

2.3 Representation Techniques for Subset Sum

For uniform random inputs, a powerful line of work accelerates meet-in-the-middle by allowing redundant encodings of a 0/1 solution using a larger coefficient alphabet (e.g., $A = \{-1, 0, 1\}$ or $A = \{-1, 0, 1, 2\}$), as summarized in Table 3.

However, there is comparatively little discussion of how such representation-based methods behave when viewed as approximators rather than exact algorithms. While representation-based algorithms implicitly discard large portions of the search space, their analyses typically focus on success probability and running

Table 1: Exact and approximate algorithms for Subset Sum (nonnegative case).

Type	Reference	Time	Space	Notes
Exact (DP)	Classical DP (Bellman '56)	$\tilde{O}(n w_{\max})$	$O(w_{\max})$	Pseudo-polynomial; $w_{\max} = \max S$
Exact (DP, randomized)	Bringmann '17	$\tilde{O}(n + T)$	$O(T)$	Near-linear randomized DP
Exact (DP, deterministic)	Koiliaris & Xu '17	$\tilde{O}(\sqrt{n} T)$ or $\tilde{O}(T^{4/3})$	$O(T)$	Subquadratic DP
FPTAS (trimming)	Kellerer & Mansini	$\tilde{O}(n + \varepsilon^{-2})$	$O(1/\varepsilon)$	Classic list trimming
FPTAS (near-linear)	Chen et al. '24	$\tilde{O}(n + 1/\varepsilon)$	$O(n + 1/\varepsilon)$	Weak scheme variant
FPTAS (trimming)	Gens & Levner '79	$O(n/\varepsilon)$	$O(1/\varepsilon)$	Empirically Fast Baseline
Exact (offset DP)	Offset-based DP	$\tilde{O}(nR)$	$O(R)$	$R = \sum_{x \in S} x $; handles negatives
Probabilistic	Ours	$O(nw \log w)$	$O(w)$ (or $O(w\sqrt{n})$ with reconstruction)	Expected error $O(B/(nw^2))$

time, rather than on how the induced approximation error decays as a function of retained state size. Because representation techniques filter partial sums using exact modular congruences, they do not naturally preserve 'close' approximations, making their direct adaptation into an expected-error heuristic non-trivial. As a result, the relationship between these techniques and expected-error frameworks has not been systematically analyzed. We view these representation-based techniques as orthogonal to our expected-error framework, rather than directly competing approaches.

2.4 Attacks on Randomized Subset Sum

RSSP admits probabilistic attacks in certain density regimes. Let the (base-2) density be $d := n/\log_2 B$. Some ranges are believed "easy," though algorithms that solve these "easy" ranges have high polynomial degree and/or rely on Shortest Vector Problem (SVP) oracles. The methods of [Lagarias and Odlyzko 1985] and [Coster et al. 1992] rely on SVP oracles.

Large density ranges remain challenging in practice, as shown in Table 4.

3 General Beam Search

Beam Search is a heuristic graph traversal algorithm that strikes a balance between breadth-first search and greedy best-first search.

Table 2: Heuristic algorithms for Subset Sum.

Method	Typical Runtime	Memory	Notes
Genetic Algorithm	$O(n \cdot \text{gen} \cdot \text{pop})$	$O(n \cdot \text{pop})$	Evolutionary, tunable
Simulated Annealing	$O(n \cdot \log T)$	$O(n)$	Escapes local minima
Particle Swarm Optimization (PSO)	$O(n \cdot \text{particles} \cdot \text{iter})$	$O(n \cdot \text{particles})$	Swarm-based
Arithmetic Optimization Algorithm (AOA)	$O(n \cdot \text{pop} \cdot \text{iter})$	$O(n \cdot \text{pop})$	Good for high density
Tabu Search	$O(n \cdot \text{iter})$	$O(n \cdot \text{tabu})$	Memory-guided local search
Hyper-heuristics	<i>Varies</i>	<i>Varies</i>	Combines multiple heuristics
Beam Search (Ours)	$O(n \cdot w \log w)$	$O(w)$ (or $O(\sqrt{n} w)$ with reconstruction)	Deterministic, proven error and variance decay

It has been used extensively in NLP tasks [Wiseman and Rush 2016] [Huang et al. 2017]. At each step, instead of expanding all possible children (as in breadth-first search), it maintains only a fixed number w of the most promising candidates—known as the *beam width*.

The algorithm proceeds in levels: at each level, every current candidate is expanded by generating its successors. All successors are scored using a heuristic function (e.g., cost, distance, or error), and only the top w are retained for the next level. This pruning mechanism reduces memory and computation compared to exhaustive methods, while preserving some diversity in the search.

Beam Search is widely used in tasks such as sequence decoding in natural language processing (e.g., machine translation), planning, combinatorial optimization, and search in large discrete spaces.

Pseudocode for Beam Search

In this formulation:

- $\text{Succ}(\text{node})$ generates all immediate successors of node.
- $\text{Score}(\text{node})$ evaluates how close a node is to the goal or optimality.
- Done returns true if the final layer of the search DAG has been reached.
- \mathcal{W} contains at most w candidates.

Beam Search is not guaranteed to find the optimal solution, but often finds high-quality approximations quickly. Its performance depends heavily on the choice of beam width and scoring heuristic [Zhou and Zhang 2020].

Table 3: Representation-based algorithms for Subset Sum (average case).

Technique	Alphabet / Params	Complexity (time / space)	Model & Reference
Baseline MITM / Schroeppe-Shamir	$A = \{0, 1\}$; 2-way split; hashing/merge	$\tilde{O}(2^{n/2})$ time; $\tilde{O}(2^{n/4})$ space	Worst case; [Horowitz and Sahni 1974; Schroeppe and Shamir 1981]
Representation + dissection (HGJ)	$A = \{-1, 0, 1\}$; modular balancing; sparse sampling	$\tilde{O}(2^{0.337n})$ time; $\tilde{O}(2^{0.337n})$ space	Uniform Random; [Howgrave-Graham and Joux 2010]
Optimized representation (BCJ)	$A = \{-1, 0, 1\}$; multi-level dissection; tuned moduli	$\tilde{O}(2^{0.291n})$ time; $\tilde{O}(2^{0.291n})$ space	Uniform Random; [Becker et al. 2011]
Larger alphabet (classical)	$A = \{-1, 0, 1, 2\}$	$\tilde{O}(2^{0.283n})$ time; $\tilde{O}(2^{0.283n})$ space	Uniform Random; [Bonnetain et al. 2020]
Larger alphabet + Grover (quantum)	$A = \{-1, 0, 1, 2\}$	$\tilde{O}(2^{0.236n})$ time; quasilinear space	Uniform Random (quantum); [Bonnetain et al. 2020]
Larger alphabet + quantum walk	$A = \{-1, 0, 1, 2\}$	$\tilde{O}(2^{0.216n})$ time; quasilinear space	Uniform Random (quantum); [Bonnetain et al. 2020]

Table 4: Density ranges where random Subset Sum is expected polynomial-time solvable.

Density regime	$\log_2 B$	Algorithm	Reference
Very low: $d < 0.6463$	$\log_2 B > 1.546n$	LLL-based lattice reduction	[Lagarias and Odlyzko 1985]
Low-Moderate: $0.6463 \leq d < 0.94$	$1.064n < \log_2 B \leq 1.546n$	Improved lattice embeddings	[Coster et al. 1992]
Quasi-polylog: $d = \Theta(n/(\log n)^2)$	$\log_2 B = O((\log n)^2)$	Recursive bit-peeling	[Flaxman and Przydatek 2005]
Very high: $d \geq \Theta(n/\log n)$	$\log_2 B = O(\log n)$	Classic pseudo-polynomial DP	—

Input: Initial state s_0 ; beam width w ; successor function $\text{Succ}(s)$; scoring function $\text{Score}(s)$; termination condition $\text{Done}(\mathcal{W})$

Output: Best state found

```

 $\mathcal{W} \leftarrow [s_0];$  // Beam: current candidates
best  $\leftarrow s_0$ ;
while  $\mathcal{W} \neq []$  and not  $\text{Done}(\mathcal{W})$  do
     $C \leftarrow [];$  // All successors
    foreach  $s \in \mathcal{W}$  do
        foreach  $s' \in \text{Succ}(s)$  do
            append  $s'$  to  $C$ ;
        end
    end
    if  $C = []$  then
        break; // No successors; dead end
    end
    sort  $C$  in descending order by  $\text{Score}(\cdot)$ ;
     $\mathcal{W} \leftarrow$  first  $\min(w, |C|)$  elements of  $C$ ; // Keep top candidates
    if  $\text{Score}(\mathcal{W}[1]) > \text{Score}(\text{best})$  then
        best  $\leftarrow \mathcal{W}[1]$ ;
    end
end
return best;

```

Algorithm 1: Generic Beam Search

3.1 Generalizing Beam Search for Subset Sum

To generalize Beam Search for the Subset Sum Problem, we treat the problem as a sequence of decisions: at each index in the input list, we can either include the element in the subset or exclude it. Each partial solution is a path in a binary tree, where each node represents a partial subset and maintains a running sum.

The algorithm proceeds iteratively, maintaining a beam of the w most promising partial solutions at each step. The score for each partial solution is determined by its absolute deviation from the target. At each step, the beam is expanded by including or excluding the next element in the list, and the top w branches (by smallest error) are retained.

Input: Set of integers $S = \{s_1, \dots, s_n\}$; target T ; beam width w

Output: Subset sum closest to T

```

 $\mathcal{W} \leftarrow \{0\}$ 
for  $i \leftarrow 1$  to  $n$  do
     $\mathcal{W} \leftarrow \mathcal{W} \cup \{x + s_i \mid x \in \mathcal{W}\}$ 
    Truncate  $\mathcal{W}$  to its  $w$  closest elements
end
return  $\arg \min_{x \in \mathcal{W}} |x - T|$ 

```

Algorithm 2: Beam Search for Closest Subset Sum

This approach requires $O(w)$ space and $O(n \cdot w \log w)$ time per run, because truncating \mathcal{W} to its w closest elements requires sorting. In practice, Beam Search provides strong empirical performance, often outperforming more complex metaheuristics in both accuracy and runtime on randomly generated subset sum instances.

4 Optimizations for Beam Search

4.1 Reconstructing the Optimal Subset

Although not the main focus of this paper, reconstructing the actual subset corresponding to the best sum is important in practice. A naive implementation keeps full parent pointers for all n layers, using $O(nw)$ memory, or recomputes layers one by one, taking $O(n^2w)$ time.

LEMMA 4.1 (INVERTIBILITY OF BEAM ITERATION). *Given the beam state $W_i \in \mathbb{R}^w$ and the step size $s_i \in \mathbb{R}$, recovering the previous beam W_{i-1} requires at least $\Omega(w)$ bits of information.*

PROOF. Given W_i and s_i , consider all possible predecessor candidates

$$W_{i-1} = W_i - s_i z_i, \quad z \in \{0, 1\}^w.$$

A candidate W_{i-1} is valid if

$$(W_{i-1} + s_i) \cup W_{i-1} = W_i.$$

Without loss of generality, assume the target value $T = 0$. Then, for each coordinate $1 \leq j \leq w$:

$$\text{if } z_j = 1, \quad |(W_{i-1})_j + s_i| \leq |(W_{i-1})_j|, \quad \text{else } |(W_{i-1})_j| \leq |(W_{i-1})_j + s_i|.$$

In words, applying the inverse operation $-z_j s_i$ should preserve the property that the chosen element remains the one closest to the target.

If $4 \max_j |(W_i)_j| \leq s_i$, then all 2^w candidates $W_{i-1} = W_i - s_i z$ satisfy the above condition, implying that W_{i-1} cannot be uniquely determined from W_i . Hence, reconstructing W_{i-1} requires at least $\Omega(w)$ bits to specify which of the 2^w possible configurations is valid. \square

Checkpointing idea. This motivates the following checkpointing approach: Every m steps we store the current beam. During reconstruction, we backtrack from the final state to the nearest checkpoint, then locally recompute at most m layers. This costs $O(w \cdot n/m)$ memory for the checkpoints and $O(wm)$ memory for the temporary recomputation. Choosing $m = \sqrt{n}$ balances the two terms, giving $O(w\sqrt{n})$ memory and $O(nw)$ time overall.

Input: Integers $S = \{s_1, \dots, s_n\}$; target T ; beam width w

Output: Best sum x^* and beam checkpoints

$m \leftarrow \lfloor \sqrt{n} \rfloor$; beam $\leftarrow \{0\}$

checkpoints $\leftarrow \{0 \mapsto \text{beam}\}$

for $i = 1$ **to** n **do**

 Expand beam with s_i and trim to width w

if $i \bmod m = 0$ **or** $i = n$ **then**

 | checkpoints[i] \leftarrow copy of beam

end

end

return best $x^* \in$ beam, checkpoints

Algorithm 3: Beam Search Forward with Checkpoints

Input: S, T, w , best sum x^* , checkpoints

Output: Indices of elements forming subset

$m \leftarrow \lfloor \sqrt{n} \rfloor$; curr_sum $\leftarrow x^*$; sol $\leftarrow \emptyset$

for $j = n$ **down to** 1 **in steps of** m **do**

 start $\leftarrow \max(0, j - m)$

 beam \leftarrow checkpoints[start]

 Recompute layers $S_{start+1}, \dots, S_j$ with parent pointers

 Backtrack from curr_sum to start, appending chosen

 indices to sol

 Update curr_sum to parent sum at start

end

Reverse sol and return

Algorithm 4: Reconstruct Subset Using Checkpoints

5 MITM Beam Search

A natural extension of the beam heuristic is to split the input into two halves and run a meet-in-the-middle (MITM) beam search. The left half generates a small set of ‘‘anchors,’’ while the right half searches against multiple residual targets. This yields a quadratic improvement in error decay.

The following analysis uses the Uniform distribution $U(0, B)$, but the algorithm is empirically robust to many input distributions.

5.1 Input Transformation

SSP can be modeled as a game of take/not take, corresponding to $1/0$. We can use this observation to formulate the following transformation: pick a random subset of elements π using a Bernoulli distribution. Then $T := T - \sum s_{\pi_i}$ and $\pi_i := -\pi_i$. For those indices we instead make the decision of not take/take. In this way, WLOG we turn any input distribution into one that is symmetric around 0.

Note that this removes the issue of sums drifting to the right over time. This means that we are now drawing elements from a symmetric distribution.

Additionally, assume T is positive; this is true WLOG by complement.

5.2 Assumptions

In the following analysis, we make the following assumptions:

- (1) All elements in the set S are drawn independently from the uniform distribution $U(-B, B)$.
- (2) The bound B is much larger than the beam width w , i.e. $B \gg w$.
- (3) The elements of S are mutually independent.
- (4) The beam width satisfies $w > 0$.
- (5) **Microscopic Offset Decorrelation (Mean-Field Heuristic):** While beam elements and anchors inherently share ancestral paths from the expansion tree, we assume their fine-scale offsets within their respective Voronoi cells act as pairwise independent continuous variables. Specifically, the dense addition of fresh i.i.d. variables at each step sufficiently mixes the least significant digits, preventing the cross-differences $Z_i - Z_j$ from collapsing into degenerate periodic lattices. This relaxation—modeling structurally dependent tree-paths as independent, well-distributed random variables to prevent degenerate state-space collapse—is

a standard heuristic in average-case Subset Sum analysis, canonically utilized in the analysis of list-merging and representation techniques [Becker et al. 2011; Howgrave-Graham and Joux 2010; Wagner 2002], and is analogous to the mean-field approximations used to analyze the Number Partitioning phase transition [Borgs et al. 2001; Mertens 1998].

5.3 Algorithm

- (1) *Phase A (anchors)*. Expand the left half, truncating after each step to one element per bucket of size B/w , choosing randomly. The resulting anchor set $A = \{a_1, \dots, a_w\}$ has maximum gap $O(B/w)$.
- (2) *Phase B (multi-target)*. For each anchor a_j define residual $r_j = T - a_j$. Before any element is within B/w of an anchor, run a width- w beam on the right half, scoring sums by distance to the residual set $\mathcal{R} = \{r_1, \dots, r_w\}$. After this, only keep one beam element per anchor region $[a_j - B/2w, a_j + B/2w]$, breaking ties within a region by distance to the representative anchor.

Phase A

Let the set of anchors at step j be

$$A_j = \{a_1^{(j)}, a_2^{(j)}, \dots, a_{|A_j|}^{(j)}\}.$$

Let $\Delta := B/w$ and let C_i denote the center of bucket i , so that bucket i corresponds to the interval

$$\mathcal{I}_i = \left[C_i - \frac{\Delta}{2}, C_i + \frac{\Delta}{2} \right].$$

At step j , bucket i is filled if there exists some $a \in A_j$ such that

$$s_j \in (\mathcal{I}_i - a) \cap [-B, B].$$

Define

$$I_{i,j} = \bigcup_{a \in A_j} ((\mathcal{I}_i - a) \cap [-B, B]).$$

Then the probability that bucket i is filled at step j is

$$\Pr(\text{bucket } i \text{ filled at step } j) = \frac{\text{Leb}(I_{i,j})}{2B}.$$

Considering only even-indexed buckets ensures that none of the intervals $\mathcal{I}_i - a$, $a \in A_j$ intersect, as each $a \in A$ will have one bucket between them, and hence have a spacing of at least B/w . Only considering even-indexed buckets can only underestimate the actual lebesgue measure. Hence, by multiplying the total size of buckets with the fraction of buckets filled, we obtain

$$\text{Leb}(I_{i,j}) \geq \Omega\left(B \cdot \frac{|A_j|}{w}\right).$$

Thus, conditioning on bucket i not yet being filled,

$$\Pr(\text{bucket } i \text{ filled at step } j \mid \text{not filled yet}) \geq \Omega\left(\frac{|A_j|}{w}\right).$$

By linearity of expectation, the expected number of new buckets filled at step j is

$$\mathbb{E}[\Delta|A_j|] = (w - |A_j|) \cdot \Omega\left(\frac{|A_j|}{w}\right).$$

Therefore, the recurrence for the expected number of anchors is

$$\mathbb{E}[|A_{j+1}|] \geq |A_j| + c(w - |A_j|) \frac{|A_j|}{w},$$

for some constant $c > 0$. Note that eliminating even anchors reduces c by a factor of $1/2$, and pessimistically considering boundary effects on $U(-B, B)$ yields another factor of $1/2$, which gives $c \geq 1/4$.

This recurrence grows geometrically, so after $O(\log w)$ steps a constant fraction of buckets will be filled.

5.3.1 Phase A: explicit bucket coverage bounds in $O(\log w)$ steps.

We now formalize the bucket-filling dynamics of Phase A and give *explicit constants* for (i) reaching half coverage in expectation, (ii) reaching essentially full coverage in expectation, and (iii) filling all buckets with high probability.

Recall the Phase A argument: after restricting to even-indexed buckets to enforce disjointness, the total reachable measure contributed by the current anchor set A_j is $\Omega(B \cdot |A_j|/w)$. Pessimistically accounting for boundary truncation to $[-B, B]$ loses another constant factor. Concretely, we obtain the following bound: conditional on a bucket i being unfilled at step j ,

$$\Pr(\text{bucket } i \text{ is filled at step } j \mid i \text{ unfilled}) \geq \frac{1}{4} \cdot \frac{|A_j|}{w}. \quad (2)$$

By linearity of expectation, the expected number of newly filled buckets satisfies

$$\mathbb{E}[\Delta|A_j|] \geq (w - |A_j|) \cdot \frac{1}{4} \frac{|A_j|}{w}.$$

Equivalently, for all j ,

$$\mathbb{E}[|A_{j+1}|] \geq |A_j| + \frac{1}{4}(w - |A_j|) \frac{|A_j|}{w}. \quad (3)$$

Let

$$x_j := \frac{\mathbb{E}[|A_j|]}{w} \in [0, 1]$$

denote the expected fraction of filled buckets. Dividing (3) by w yields the discrete logistic drift inequality

$$x_{j+1} - x_j \geq \frac{1}{4} x_j (1 - x_j). \quad (4)$$

Continuous comparison. The inequality (4) is naturally compared to the logistic ODE

$$\frac{dx}{dt} = \frac{1}{4} x(1 - x), \quad x(0) = x_0, \quad (5)$$

whose explicit solution is

$$x(t) = \frac{1}{1 + \left(\frac{1}{x_0} - 1\right) e^{-t/4}}. \quad (6)$$

With $x_0 = 1/w$ (since $|A_0| = 1$), this becomes

$$x(t) = \frac{1}{1 + (w - 1) e^{-t/4}}. \quad (7)$$

LEMMA 5.1 (HALF COVERAGE IN EXPECTATION). *There exists an explicit iteration index*

$$j_{\text{half}} \leq 4 \ln(w - 1) \leq 4 \ln w$$

such that

$$\mathbb{E}[|A_{j_{\text{half}}}|] \geq \frac{w}{2}.$$

Input: Integers $S = \{s_1, \dots, s_n\}$, target T , beam width w , bound B
Output: Best right-half sum x^* minimizing distance to residuals

```

 $n_L \leftarrow \lceil C \log w \rceil;$ 
 $S_L \leftarrow (s_1, \dots, s_{n_L}); \quad S_R \leftarrow (s_{n_L+1}, \dots, s_n);$ 

Phase A (anchors from left half via one-per-bucket);
 $\Delta \leftarrow B/w;$  // bucket width on  $[-B/2, B/2]$ 
 $\mathcal{W} \leftarrow \{0\};$ 
for  $i = 1$  to  $n_L$  do
  expanded  $\leftarrow \mathcal{W} \cup \{x + s_i : x \in \mathcal{W}\};$ 
   $E \leftarrow \{x \in \text{expanded} : -B/2 \leq x \leq B/2\};$ 
  // Partition  $[-B/2, B/2]$  into  $w$  half-open buckets  $\mathcal{I}_j$ 
   $\mathcal{W} \leftarrow \emptyset;$ 
  for  $j = 1$  to  $w$  do
     $\mathcal{I}_j \leftarrow [-B/2 + (j-1)\Delta, -B/2 + j\Delta);$ 
     $C_j \leftarrow \{x \in E : x \in \mathcal{I}_j\};$ 
    if  $C_j \neq \emptyset$  then
      pick  $x$  uniformly at random from  $C_j$ ;
       $\mathcal{W} \leftarrow \mathcal{W} \cup \{x\};$ 
    end
  end
end
 $A \leftarrow \mathcal{W};$ 
 $\mathcal{R} \leftarrow \{T - a : a \in A\};$  // residual targets for right half
Delete even-indexed anchors

Phase B (right half: residual-guided, then one-per-anchor);
 $\mathcal{W} \leftarrow \{0\};$ 
for  $i = n_L + 1$  to  $n$  do
  expanded  $\leftarrow \mathcal{W} \cup \{x + s_i : x \in \mathcal{W}\};$ 
  // Distance to residual set
  foreach  $x \in \text{expanded}$  do
     $d(x) \leftarrow \min_{r \in \mathcal{R}} |x - r|;$ 
  end
  // Detect whether we have entered the anchor neighborhood regime
   $H \leftarrow \{x \in \text{expanded} : d(x) \leq \Delta\};$ 
  if  $H = \emptyset$  then
    // Pre-hit regime: keep the  $w$  closest sums to residuals
     $\mathcal{W} \leftarrow$  the  $w$  elements of expanded with smallest  $d(x)$ ;
  else
    // Post-hit regime: one-per-anchor over Voronoi cells of  $\mathcal{R}$ 
    foreach  $x \in \text{expanded}$  do
       $r(x) \leftarrow \arg \min_{r \in \mathcal{R}} |x - r|;$  // closest-anchor assignment; break ties arbitrarily
    end
     $\mathcal{W} \leftarrow \emptyset;$ 
    foreach  $r \in \mathcal{R}$  do
       $C_r \leftarrow \{x \in \text{expanded} : r(x) = r\};$ 
      if  $C_r \neq \emptyset$  then
        // Keep the best representative inside anchor  $r$ 's Voronoi region
        pick  $x_r \in \arg \min_{x \in C_r} |x - r|;$  // ties arbitrary (or random)
         $\mathcal{W} \leftarrow \mathcal{W} \cup \{x_r\};$ 
      end
    end
  end
end
 $x^* \leftarrow \arg \min_{x \in \mathcal{W}} d(x);$ 
return  $x^*;$ 

```

Algorithm 5: MITM Beam Search (bucketed anchors + residual-guided right-half beam)

Equivalently, Phase A reaches half coverage in at most

$$j_{\text{half}} \leq 4 \ln w = (4 \ln 2) \log_2 w \leq 2.773 \log_2 w$$

steps.

PROOF. Setting $x(t) = 1/2$ in (7) yields $(w-1)e^{-t/4} = 1$, i.e. $t = 4 \ln(w-1)$. The stated bounds follow from $\ln(w-1) \leq \ln w$ and $\ln w = (\ln 2) \log_2 w$. \square

Geometric contraction after half coverage. For $x_j \geq 1/2$, define the expected unfilled fraction $u_j := 1 - x_j$. From (4),

$$x_{j+1} - x_j \geq \frac{1}{4} \cdot \frac{1}{2} u_j = \frac{1}{8} u_j,$$

which implies

$$u_{j+1} \leq \frac{7}{8} u_j. \quad (8)$$

Thus, once half the buckets are filled, the remaining unfilled mass contracts geometrically at rate $7/8$ per step.

LEMMA 5.2 (ESSENTIALLY FULL COVERAGE IN EXPECTATION). Let j_{half} be as in Lemma 5.1 and define

$$t_{\text{exp}} := \left\lceil \frac{\ln(w/2)}{\ln(8/7)} \right\rceil, \quad j_{\text{all,exp}} := j_{\text{half}} + t_{\text{exp}}.$$

Then the expected number of unfilled buckets is at most one:

$$\mathbb{E}[w - |A_{j_{\text{all,exp}}}|] \leq 1.$$

Moreover, using $\ln(8/7) \approx 0.13353$ (so $1/\ln(8/7) \approx 7.489$), we obtain the explicit bound

$$\begin{aligned} j_{\text{all,exp}} &\leq 4 \ln w + \frac{\ln(w/2)}{\ln(8/7)} + 1 \leq \left(4 + \frac{1}{\ln(8/7)}\right) \ln w + 1 \\ &\leq 11.489 \ln w + 1 = (11.489 \ln 2) \log_2 w + 1 \leq 7.96 \log_2 w + 1. \end{aligned}$$

PROOF. At time j_{half} we have $u_{j_{\text{half}}} \leq 1/2$. Applying (8) for t additional steps yields

$$\mathbb{E}[w - |A_{j_{\text{half}}+t}|] = w u_{j_{\text{half}}+t} \leq \frac{w}{2} \left(\frac{7}{8}\right)^t.$$

Choosing $t = t_{\text{exp}}$ makes the right-hand side at most 1. The numerical constants follow from $1/\ln(8/7) \approx 7.489$ and $\ln 2 \approx 0.6931$. \square

THEOREM 5.3 (ALL BUCKETS FILLED WITH HIGH PROBABILITY). Fix $\delta \in (0, 1)$. Let

$$t_\delta := \left\lceil \frac{\ln(w/(2\delta))}{\ln(8/7)} \right\rceil, \quad j_\delta := j_{\text{half}} + t_\delta.$$

Then

$$\Pr(|A_{j_\delta}| < w) \leq \delta,$$

i.e., Phase A fills all buckets with probability at least $1 - \delta$ by iteration j_δ .

Moreover, using $1/\ln(8/7) \approx 7.489$, we have the explicit bound

$$\begin{aligned} j_\delta &\leq 4 \ln w + \frac{\ln(w/(2\delta))}{\ln(8/7)} + 1 \leq \left(4 + \frac{1}{\ln(8/7)}\right) \ln w + \frac{\ln(1/\delta)}{\ln(8/7)} + 1 \\ &\leq 11.489 \ln w + 7.489 \ln(1/\delta) + 1 \\ &= 7.96 \log_2 w + 5.19 \log_2(1/\delta) + 1. \end{aligned}$$

In particular, for any fixed constant δ (e.g., $\delta = 0.01$), this is $j_\delta \leq 11.489 \ln w + O(1)$.

PROOF. By Lemma 5.2, for any $t \geq 0$,

$$\mathbb{E}[w - |A_{j_{\text{half}}+t}|] \leq \frac{w}{2} \left(\frac{7}{8}\right)^t.$$

Markov's inequality gives

$$\Pr(|A_{j_{\text{half}}+t}| < w) = \Pr(w - |A_{j_{\text{half}}+t}| \geq 1) \leq \mathbb{E}[w - |A_{j_{\text{half}}+t}|] \leq \frac{w}{2} \left(\frac{7}{8}\right)^t.$$

Choosing $t = t_\delta$ makes the right-hand side at most δ . The numerical constants follow as above. \square

Consequence: mesh size. Once all buckets are filled, selecting one anchor per bucket yields a mesh with maximum gap $O(B/w)$. Deleting every even-indexed bucket ensures both minimum and maximum gaps are $\Theta(B/w)$.

Consequence: meshing in linearithmic time. Phase A fills all buckets in $O(\log w)$ steps w.h.p. with explicit constants. For fixed δ , Lemma 5.3 gives

$$j_\delta \leq 11.489 \ln w + O(1) = 7.96 \log_2 w + O(1).$$

Since each iteration maintains at most $O(w)$ candidates, the mesh is constructed in expected $O(w \log w)$ time.

Comparison to prior work. In our work, we consider a parameter w controlling the fineness of the mesh. In the worst case, assuming all buckets are filled, any $x \in [-B/2, B/2]$ would be at most $\Delta = \frac{B}{w}$ away from an anchor.

Da Cunha et al. [Da Cunha et al. 2023] show that given n independent uniform variables $X_1..X_n$, $X_i \in [-1, 1]$, and a constant parameter $\epsilon \in (0, 1/3)$, with probability of at least $1 - \epsilon$, for all $z \in [-1, 1]$, there exists a subset S of $X_1..X_n$ such that $|\sum_{i \in S} X_i - z| \leq \epsilon$ if $n = O(\log(1/\epsilon))$. This can be restated equivalently as:

Given n independent uniform variables $X_1..X_n$, $X_i \in [-B, B]$, and a constant parameter $w \in (3, \infty)$, with probability of at least $1 - 1/w$, for all $z \in [-B, B]$, there exists a subset S of $X_1..X_n$ such that $|\sum_{i \in S} X_i - z| \leq B/w$ if $n = O(\log w)$.

If one were to naively materialize the full binary expansion tree to depth $O(C \log w)$, the number of generated partial sums would be

$$2^{O(C \log w)} = w^{O(C)}.$$

In contrast, our Phase A construction enforces width w throughout via bucketing and trimming at every level, and we prove that all w buckets are filled with probability at least $1 - \delta$ within

$$j_\delta \leq 7.96 \log_2 w + 5.19 \log_2(1/\delta) + 1$$

iterations (Lemma 5.3). The ability to construct a mesh on an interval $[-B/2, B/2]$ given starting element zero offers a construction to extend to $[-B, B]$, although this is usually not necessary: Build a mesh on $[-B/2, B/2]$, find the minimum anchor in the mesh $a_{\min} \leq -B/2 - B/w$, then build a mesh on $[a_{\min} - B/2, a_{\min} + B/2]$. Find the minimum on this mesh $a'_{\min} \leq B - 2B/w$, creating another mesh $[a'_{\min} - B/2, a'_{\min} + B/2]$. For $w \geq 4$ the union of these meshes will fully cover $[-B, 0]$. Repeat symmetrically for positive side, for a pessimistic additional constant factor of 5.

Consequently, the mesh is constructed in $O(w \log w)$ time while maintaining $O(w)$ state.

For any fixed failure probability δ (e.g. $\delta = 0.01$), the leading constant on $\log_2 w$ is explicit and below 10 ($7.96 \log_2 w + O(1)$),

whereas the result of Da Cunha et al. does not provide an explicit, bounded constant for a width- w trimmed construction.

This result strengthens proofs that rely on the results of Da Cunha et al, such as the proof of the Strong Lottery Ticket Hypothesis [Frankle et al. 2020].

LEMMA 5.4 (UNIFORMITY WITHIN A BUCKET). *Fix a time step t and a bucket $\mathcal{I}_i \subseteq [-B/2, B/2]$ with $0 \notin \mathcal{I}_i$. Let $E_{t,i}$ be the multiset of candidate anchors that fall in \mathcal{I}_i at time t , i.e.,*

$$E_{t,i} := \{p + s_t : p \in A^{(t-1)}, p + s_t \in \mathcal{I}_i\},$$

where $s_t \sim U([-B, B])$ is independent of $A^{(t-1)}$. If the algorithm selects a by choosing an element uniformly at random from $E_{t,i}$ (conditioned on $E_{t,i} \neq \emptyset$), then

$$a \mid (a \in \mathcal{I}_i, E_{t,i} \neq \emptyset) \sim U(\mathcal{I}_i).$$

PROOF. Condition on $A^{(t-1)}$ and on the event that a specific parent $p \in A^{(t-1)}$ produces a candidate in \mathcal{I}_i , i.e. on the event

$$F_p := \{p + s_t \in \mathcal{I}_i\} \equiv \{s_t \in \mathcal{I}_i - p\}.$$

Because $s_t \sim U([-B, B])$ and $\mathcal{I}_i \subseteq [-B/2, B/2]$ while $p \in [-B/2, B/2]$ (by construction of Phase A), we have $\mathcal{I}_i - p \subseteq [-B, B]$. Therefore, conditioning on F_p yields

$$s_t \mid F_p \sim U(\mathcal{I}_i - p).$$

By translation, this implies

$$p + s_t \mid F_p \sim U(\mathcal{I}_i).$$

Now condition only on the event that the bucket is nonempty, $E_{t,i} \neq \emptyset$. Each element of $E_{t,i}$ arises from some parent p and, conditional on its existence, has distribution $U(\mathcal{I}_i)$ as shown above. The algorithm selects uniformly among the (random number of) elements in $E_{t,i}$, so the selected a is a mixture of $U(\mathcal{I}_i)$ distributions with mixing weights that sum to 1. A mixture of identical distributions is the same distribution; hence $a \sim U(\mathcal{I}_i)$. \square

Phase B

Let \mathcal{W} denote the Phase B beam. Assume Phase A has filled a constant fraction of buckets, and for simplicity that all buckets are filled. This happens in $O(\log w)$ steps, as proven in Phase A analysis. To simplify analysis, we delete every even-indexed bucket; this guarantees anchors are separated by $\Theta(B/w)$ and that the mesh (maximum spacing) is also $\Theta(B/w)$. This is done because each bucket has length $O(B/w)$ so having no two adjacent buckets guarantees at least that much spacing. Deleting every other bucket can only reduce maximum spacing by a constant factor, and with all buckets filled max spacing was $O(B/w)$.

Without this deletion, anchors could cluster at bucket edges, complicating the spacing guarantees.

Define

$$Z = \{T - a_i : a_i \in A\}.$$

For any $x \in \mathcal{W}$, its distance to Z is

$$d(x) = \min_{z \in Z} |x - z|.$$

If $d(x) = d$, then choosing a shift $s \sim U([-B, B])$ that lands in $[z - d, z + d]$ for some $z \in Z$ reduces the error to at most $d' < d$.

—

Burn-in to the small-gap regime. Before the expected error decay can take effect, the beam must reach the target range and populate the anchor Voronoi cells. We call this the “burn-in” period.

LEMMA 5.5 (BURN-IN DURATION). *Assume Phase A has filled all buckets, yielding an anchor set Z spaced by $\Theta(B/w)$. With high probability, every anchor Voronoi cell will be occupied by at least one beam element after*

$$t_{burn} = O\left(\frac{\min Z}{B}\right) + O(\log w).$$

steps.

PROOF SKETCH. The burn-in occurs in two distinct phases:

- (1) **Reaching the anchor range:** Before entering the target range $Q = [\min Z - c\frac{B}{w}, \max Z + c\frac{B}{w}]$, the beam scoring strictly preserves the largest values. The beam evolves as a random walk with positive drift. By a standard Central Limit Theorem argument, the beam enters Q in $O(\min Z/B)$ steps.
- (2) **Filling Voronoi cells:** Once inside Q , the multi-target scoring ensures that when a Voronoi cell is occupied, it cannot become vacant again. The filling of the remaining unoccupied cells follows the exact same discrete logistic drift dynamics as Phase A (see Section 5.3.1). Consequently, all $m = \Theta(w)$ cells are filled in an additional $O(\log w)$ steps.

The rigorous proofs establishing error monotonicity, filling monotonicity, and the formal logistic drift lower bound are deferred to Appendix C. \square

Single element analysis. Fix a beam element x at distance $d(x) = d$ from Z .

Probability of improvement. - Each anchor $z \in Z$ contributes an interval $[z - d, z + d]$ of length $2d$. - Because anchors are $\Omega(B/w)$ apart, for Lebesgue measure calculations, these intervals can be considered disjoint, up to constant factors. - There are $\Theta(w)$ anchors within range B (since spacing is $\Theta(B/w)$, and the whole domain has length $2B$). - Thus the total “improvement region” has length $\Theta(wd)$. - Since $s \sim U([-B, B])$, the probability of improvement is

$$\Pr(\text{improvement} \mid d) = \Theta\left(\min\left\{1, \frac{wd}{B}\right\}\right).$$

LEMMA 5.6. *Conditional on an improvement occurring, the new minimum gap D' is stochastically dominated by a uniform distribution on $[0, D]$. That is, conditional on improvement, the expected new gap satisfies $\mathbb{E}[D'] \leq \frac{D}{2}$.*

PROOF. For each pair (i, k) of beam element x_i and anchor Z_k , an improvement occurs if the shift s falls within the interval $[Z_k - x_i - D, Z_k - x_i + D]$, which has length $2D$. On any such single interval, the mapping

$$s \mapsto |(x_i + s) - Z_k|.$$

is piecewise linear, and its image is exactly $[0, D]$. Because s is drawn uniformly from $[-B, B]$, if s falls into exactly one such improvement interval, the resulting new gap is exactly uniform on $[0, D]$.

In the case where multiple improvement intervals overlap, s may fall into an intersection of two or more intervals. When this happens, the new global minimum gap D' is the minimum over all pairs (i, k)

for which s is an improving shift. Since taking the minimum of multiple variables can only decrease the final value, the resulting distribution of D' is stochastically smaller than $U(0, D)$. Therefore, overlapping intervals strictly improve the error decay, and we can safely upper-bound the expected new gap by the expectation of a $U(0, D)$ variable, yielding $\mathbb{E}[D'] \leq \frac{D}{2}$. \square

Expected drift. Let D_t be the global minimum gap at step t , where D_0 is the minimum gap right after Burn-in, and hence $D_0 \leq B/w$.

Because we are bounding the expected remaining error from above, the gap shrinks by at least:

$$\mathbb{E}[D_{t+1} - D_t \mid D_t = D] \leq -c \frac{w}{B} D^2$$

for some absolute constant $c > 0$.

Discrete Decay Bound. By definition, after burn-in, the initial gap satisfies $D_0 \leq B/w$. Setting $k = c \frac{w}{B}$, we have $kD_0 \leq c$. By absorbing constants into the base step if necessary, we can ensure the strict condition $kD_0 < 1$ is met to apply the following inductive bound.

LEMMA 5.7 (DISCRETE DECAY ERROR BOUND). *Assume the expected gap is bounded by the discrete recursion envelope*

$$D_{t+1} = D_t - kD_t^2,$$

where $k = c \frac{w}{B}$ and the initial state satisfies $kD_0 < 1$. Then $D_t = O(\frac{B}{wt})$.

PROOF. Rearranging this recursion yields:

$$\frac{1}{D_{t+1}} = \frac{1}{D_t(1 - kD_t)} \geq \frac{1}{D_t} + k,$$

where the inequality follows from the geometric series expansion of $(1 - kD_t)^{-1}$. This expansion is strictly valid because $kD_t \leq kD_0 < 1$. By induction over t steps, this yields:

$$\frac{1}{D_{t+1}} \geq \frac{1}{D_0} + k(t+1) \implies D_{t+1} \leq \frac{D_0}{1 + kD_0(t+1)}.$$

Substituting $k = c \frac{w}{B}$ back into the bound, we obtain:

$$D_{t+1} \leq \frac{D_0}{1 + c \frac{wD_0}{B}(t+1)} = \frac{1}{\frac{1}{D_0} + c \frac{w}{B}(t+1)}.$$

Using the initial bound $D_0 \leq B/w$, we know $\frac{1}{D_0} \geq \frac{w}{B}$. Substituting this into the denominator strictly upper-bounds the fraction, yielding:

$$D_{t+1} \leq \frac{1}{\frac{w}{B} + c \frac{w}{B}(t+1)} = \frac{1}{\frac{w}{B}(1 + c(t+1))}.$$

Since $c > 0$ is a constant, this simplifies directly to the asymptotic bound:

$$D_t = O\left(\frac{B}{wt}\right),$$

yielding the stated decay rate. \square

LEMMA 5.8. *Deterministic Recursion Overestimates Error Compared to Stochastic Recursion The deterministic recursion*

$$D_{t+1} = D_t - kD_t^2$$

can only overestimate the error compared to the stochastic version

$$\mathbb{E}[D_{t+1} \mid D_t] \leq D_t - kD_t^2.$$

PROOF. We proceed by analyzing the unconditional expectation of the stochastic drift. Taking the expectation of both sides with respect to the filtration up to time t yields:

$$\mathbb{E}[D_{t+1}] \leq \mathbb{E}[D_t] - k\mathbb{E}[D_t^2].$$

Because the function $f(x) = x^2$ is strictly convex, we apply Jensen's inequality, which guarantees that the expectation of the square is bounded below by the square of the expectation: $\mathbb{E}[D_t^2] \geq (\mathbb{E}[D_t])^2$.

Since $k > 0$, substituting this lower bound into the subtracted term strictly upper-bounds the right-hand side:

$$\mathbb{E}[D_{t+1}] \leq \mathbb{E}[D_t] - k(\mathbb{E}[D_t])^2.$$

Let $y_t = \mathbb{E}[D_t]$ represent the expected error at step t . The sequence of expectations satisfies the recurrence inequality:

$$y_{t+1} \leq y_t - ky_t^2.$$

Now, consider the deterministic sequence z_t defined by the exact recurrence $z_{t+1} = z_t - kz_t^2$, initialized at $z_0 = y_0 = \mathbb{E}[D_0]$.

Because $D_t \geq 0$ almost surely, $y_t \geq 0$. Provided the initial state satisfies the stability condition $2kz_t < 1$ (which guarantees the mapping $x \mapsto x - kx^2$ is strictly monotonically increasing on the relevant domain), we can proceed by induction. Assume $y_t \leq z_t$; then:

$$y_{t+1} \leq y_t - ky_t^2 \leq z_t - kz_t^2 = z_{t+1}.$$

Therefore, $\mathbb{E}[D_t] \leq z_t$ for all $t \geq 0$. Because the stochastic variance term ($\text{Var}(D_t) = \mathbb{E}[D_t^2] - (\mathbb{E}[D_t])^2$) is strictly non-negative, the stochastic sequence will, in expectation, decay faster than its deterministic counterpart. Thus, the deterministic ODE or discrete envelope serves as a rigorous upper bound for the expected stochastic error. \square

Multiple Elements. Let the minimum distance of the w beam elements to any anchor be D .

At step j , the gap D improves iff

$$x_i + s_j \in \bigcup_{k=1}^w [Z_k - D, Z_k + D] =: A \quad \text{for some } i \in [w],$$

or equivalently

$$s_j \in \bigcup_{i=1}^w (A - x_i).$$

Hence, the probability of improvement relies on the total Lebesgue measure of this union:

$$\Pr(\text{improvement from } D) = \frac{\text{Leb}(\bigcup_{i=1}^w (A - x_i) \cap [-B, B])}{2B}.$$

Because Phase A and Phase B are generated via tree expansions, the precise joint distribution of the anchors Z and the beam elements x contains path dependencies. However, to evaluate the expected volume of the improvement region, we only require that the w^2 pairwise differences $Z_k - x_i$ do not perfectly overlap. Under **Assumption 5**, the local offsets of these elements are sufficiently decorrelated such that we can treat them as pairwise independent for the purpose of the union bound, preventing a state-space collapse.

LEMMA 5.9 (ANCHOR CONVOLUTION UNION: EXPECTATION LOWER BOUND). *Partition $[-B/2, B/2]$ into w buckets of length $\Delta := \frac{B}{w}$. Under Assumption 5, let the anchors and beam elements be modeled as:*

$$Z_i^{(1)} = C_i + U_i, \quad Z_j^{(2)} = C_j + U_j + D_j,$$

where $C_i = -B/2 + \left(i - \frac{1}{2}\right)\Delta$, the variables $U_i, U_j \sim \text{Unif}[-\Delta/2, \Delta/2]$ represent the pairwise-decorrelated microscopic offsets, and D_j are arbitrary random variables supported on $[-\Delta/2, \Delta/2]$ representing the current gap.

Define the cross-differences $D_{ij} = Z_i^{(1)} - Z_j^{(2)}$ and the union of improvement intervals:

$$\mathcal{U}_d = \bigcup_{i,j=1}^w [D_{ij} - d, D_{ij} + d].$$

There exist absolute constants $c, c' > 0$ such that if $d \leq c \frac{\Delta}{w}$, then the expected measure avoids degenerate collapse and scales quadratically with w :

$$\mathbb{E}[\text{Leb}(\mathcal{U}_d)] \geq c' w^2 d.$$

PROOF. Write the cross-difference as:

$$D_{ij} = (C_i - C_j) + (U_i - U_j) - D_j.$$

Group pairs (i, j) by the macroscopic diagonal offset $s = i - j \in \{-(w-1), \dots, w-1\}$. For a fixed s , the deterministic macroscopic distance $C_i - C_{i-s} = s\Delta$ is constant, leaving the microscopic jitter governed strictly by $(U_i - U_{i-s}) - D_{i-s}$. Because Assumption 5 grants pairwise independence to the offsets U , the distribution of $(U_i - U_{i-s})$ forms a non-degenerate convolution (a triangular distribution of width 2Δ).

The number of pairs for a given s is $M_s = w - |s|$. For any $|s| \leq w/2$, we have $M_s = \Theta(w)$. Since the centers D_{ij} are independently and continuously smeared across intervals of width 2Δ , the expected intersection length of any two distinct target intervals E_a and E_b on the same diagonal is strictly bounded by their convolution: $\mathbb{E}[\text{Leb}(E_a \cap E_b)] = O(d^2/\Delta)$. Applying the second-moment Bonferroni inequality, the expected measure of the union is bounded below by the sum of individual expected lengths minus the sum of pairwise expected intersections:

$$\mathbb{E}\left[\text{Leb}\left(\bigcup_{k=1}^{M_s} E_k\right)\right] \geq \sum_{k=1}^{M_s} 2d - \sum_{a < b} O\left(\frac{d^2}{\Delta}\right) = 2M_s d - O\left(M_s^2 \frac{d^2}{\Delta}\right).$$

Given the condition $d \leq c \frac{\Delta}{w}$ and $M_s \leq w$, the subtracted intersection term simplifies to $O\left(M_s d \cdot \frac{wd}{\Delta}\right) \leq O(M_s d \cdot c)$. By choosing the constant c sufficiently small, the dominant linear sum is strictly preserved, yielding $\Omega(M_s d)$ per diagonal. Summing across the $\Theta(w)$ primary diagonals yields the global lower bound $\mathbb{E}[\text{Leb}(\mathcal{U}_d)] = \Omega(w^2 d)$. \square

Connection to the improvement probability. Let D be the current minimum beam–anchor distance. Improvement occurs iff

$$s \in \bigcup_{i=1}^w (A(D) - x_i) \cap [-B, B], \quad A(D) = \bigcup_{k=1}^w [Z_k - D, Z_k + D].$$

First, after burn-in, every V_j is occupied by at least one element, implying that every anchor has an associated beam element attached to it.

Second, by Lemma 5.4, each anchor satisfies $Z_k = C_k + U_k$ with U_k uniform within its bucket.

Thirdly, by Lemma 5.6, when a beam element with original distance d attaches to an anchor, its new distance is rolled as $U(0, d)$, independently from the new anchor. By the single-element analysis, d will shrink below $\frac{\Delta}{2}$ in $O(1)$ steps. This can be pessimistically replaced by $\mathcal{D}(0, \Delta/2)$, where \mathcal{D} is an arbitrary distribution. Using offset rather than absolute distance yields $\mathcal{D}(-\Delta/2, \Delta/2)$.

Hence we may pessimistically beam element x_i as follows:

$$\tilde{x}_i = Z_{j(i)} + \mathcal{D}(-\Delta/2, \Delta/2) = C_{j(i)} + U_{j(i)} + \mathcal{D}(-\Delta/2, \Delta/2),$$

where $j(i)$ is the index of the anchor that beam element x_i is attached to. $U_i \sim \text{Unif}[-\Delta/2, \Delta/2]$, and \mathcal{D} is an arbitrary distribution, independent from $U_{j(i)}$.

Renaming $Z^{(1)} := Z$ and $Z_i^{(2)} = C_j + U_j + \mathcal{D}(-\Delta/2, \Delta/2)$ allows direct substitution into Lemma 5.9, yielding

$$\mathbb{E}\left[\text{Leb}\left(\bigcup_{i=1}^w (A(D) - x_i) \cap [-B, B]\right)\right] \geq c' w^2 D.$$

Dividing by B gives

$$\text{Pr}(\text{improvement from } D) \geq \Theta\left(\frac{w^2 D}{B}\right), \quad D \ll B/w^2.$$

If $D > \frac{B}{w^2}$, note that the improvement Lebesgue measure trivially grows monotonically with D . Hence, when $D > \frac{B}{w^2}$,

$$\mathbb{E}\left[\text{Leb}\left(\bigcup_{i=1}^w (A(D) - x_i) \cap [-B, B]\right)\right] \geq c' w^2 \frac{B}{w^2} = c' B,$$

which yields

$$\text{Pr}(\text{improvement from } D) \geq \Omega(1), \quad D > B/w^2,$$

which causes D to shrink geometrically until $D \ll \frac{B}{w^2}$.

Discrete recursion and transition. In the saturated subregime (when $D \gtrsim B/w^2$), the probability of improvement is $\Omega(1)$, causing the gap to decay geometrically by at least a constant factor per step. After at most $T_{\text{sat}} = O(\log w)$ steps, the process enters the small-gap regime where $D_{T_{\text{sat}}} \ll B/w^2$.

Once in the small-gap regime, the expected gap shrinks by at least $c' \frac{w^2}{B} D^2$ per step. We define our discrete recurrence constant as $k = c' \frac{w^2}{B}$. Because $D_{T_{\text{sat}}} \ll B/w^2$, the entry condition $k D_{T_{\text{sat}}} < 1$ is strictly satisfied. By substituting this k into Lemma 5.7 and applying to the stochastic version with Lemma 5.8, we obtain an upper bound on the error of:

$$D_t \leq O\left(\frac{B}{w^2(t - T_{\text{sat}})}\right) = O\left(\frac{B}{w^2 t}\right).$$

THEOREM 5.10 (PHASE B INVERSE-QUADRATIC EXPECTED ERROR DECAY). *Consider Phase B of the MITM beam search with beam width w and anchors constructed by Phase A. Assume the burn-in conditions hold, i.e., after an initial burn-in of*

$$t_0 = O\left(\frac{\min Z}{B}\right) + O(\log w)$$

steps, every anchor Voronoi cell is occupied by at least one beam element.

Let D_t denote the minimum distance of the Phase B beam to the residual anchor set Z at time $t \geq t_0$. Then there exists an absolute constant $c > 0$ such that for all $t \geq t_0$,

$$\mathbb{E}[D_t] \leq \frac{cB}{w^2(t-t_0+1)}.$$

Equivalently, up to constant factors,

$$\mathbb{E}[D_t] = O\left(\frac{B}{w^2 t}\right).$$

Moreover, the standard deviation satisfies

$$\text{sd}(D_t) = \Theta(\mathbb{E}[D_t]),$$

with the variance bound proven in Appendix A.

PROOF SKETCH. After burn-in, every anchor Voronoi cell is occupied. By Lemma 5.9, the probability of improvement from distance D_t is $\Theta(w^2 D_t / B)$ in the small-gap regime, and bounded below by a constant when $D_t \gtrsim B/w^2$.

Conditional on improvement, Lemma 5.6 shows the new gap is uniformly distributed on $[0, D_t]$, yielding

$$\mathbb{E}[D_{t+1} - D_t \mid D_t] = -\Theta\left(\frac{w^2}{B}\right) D_t^2.$$

Applying the discrete bounds from Lemma 5.7 via the stochastic comparison in Lemma 5.8 implies

$$D_t \leq O\left(\frac{B}{w^2 t}\right),$$

and the stated variance scaling follows from Appendix A. \square

THEOREM 5.11 (END-TO-END MITM BEAM GUARANTEE). Let $S = \{s_1, \dots, s_n\}$ be i.i.d. samples from a symmetric distribution supported on $[-B, B]$, and let T be a target generated as the sum of a subset of S . Fix beam width w .

Run the MITM beam search with:

- Phase A using $n_L = \Theta(\log w + \log(1/\delta))$ elements to construct anchors, and
- Phase B on the remaining $n_R = n - n_L$ elements.

Burn-in duration and worst-case targets. The total number of elements consumed before Phase B is $n_{pre} = n_L + t_{burn}$, which evaluates to:

$$n_{pre} = O(\log w) + O(\log(1/\delta)) + \frac{4 \min Z}{B} + O\left(\sqrt{\frac{\min Z}{B}}\right) = \frac{4 \min Z}{B} + o(n).$$

Because $\min Z \leq T$, the survival of Phase B depends entirely on the magnitude of the target T . However, we now prove that $n - n_{pre} = \Theta(n)$, unless the instance is solvable in subexponential time.

Let $S_{max} = \sum_{s_i > 0} s_i$ denote the maximum possible subset sum. Because $s_i \sim U([-B, B])$, the expected value of S_{max} is $nB/4$. By Hoeffding's inequality (or CLT), S_{max} concentrates tightly, so $S_{max} = \frac{nB}{4} \pm o(nB)$ with overwhelming probability. Since T is a valid subset sum, $T \leq S_{max}$. We divide the target space into two regimes based on an arbitrarily small constant $\gamma \in (0, 1/4)$:

Case 1: Strictly bounded targets ($T \leq (1/4 - \gamma)nB$). In this regime, the elements consumed before Phase B are strictly bounded by $n_{pre} \leq (1 - 4\gamma)n + o(n)$. This leaves $n_R \geq 4\gamma n - o(n) = \Theta(n)$ elements for Phase B. Because the number of available Phase B steps remains linear with respect to n , the expected error decay strictly preserves the

asymptotic bound of $O\left(\frac{B}{n_R w^2}\right) = O\left(\frac{B}{nw^2}\right)$, absorbing the constant $\frac{1}{4\gamma}$ into the asymptotic notation.

Case 2: Extreme maximum targets ($T > (1/4 - \gamma)nB$). If the target is chosen adversarially close to S_{max} , the burn-in may consume $n_{pre} = n - o(n)$ elements, starving Phase B. However, in this regime, the problem undergoes a severe state-space collapse. Define the residual slack as $\epsilon = S_{max} - T$. Because T is extremely large, $\epsilon = o(nB)$.

To achieve a sum of T , the optimal subset must be formed by taking the maximal configuration and making deviations (either excluding a positive element or including a negative element). Every such deviation consumes a portion of the slack ϵ equal to the magnitude of the element. Consider the set of "large" elements, $L = \{s_i \in S \mid |s_i| \geq B/2\}$. The expected size of L is exactly $n/2 = \Theta(n)$.

Because each deviation in L consumes at least $B/2$ slack, the maximum number of deviations we can make among the large elements is bounded by:

$$k_{deviations} \leq \frac{\epsilon}{B/2} = \frac{o(nB)}{B/2} = o(n).$$

Therefore, out of the $\Theta(n)$ large elements, at most $o(n)$ can deviate from the maximal configuration. This guarantees that the inclusion/exclusion status of $\Theta(n) - o(n) = \Theta(n)$ elements is deterministically forced. The effective number of undecided elements drops to $o(n)$, allowing the residual problem to be solved exactly via brute-force enumeration or standard dynamic programming in subexponential time.

Thus, across all valid targets, the algorithm either achieves the $O\left(\frac{B}{nw^2}\right)$ error bound via the beam search decay, or the instance collapses into a trivially solvable subexponential state.

Hence, with probability at least $1 - \delta$,

$$\mathbb{E}[|S^* - T|] = O\left(\frac{B}{nw^2}\right), \quad \text{sd}(|S^* - T|) = \Theta(\mathbb{E}[|S^* - T|]).$$

The algorithm runs in $O(nw \log w)$ time and $O(w)$ memory. Exact subset reconstruction is supported in $O(nw)$ time using $O(w\sqrt{n})$ memory via checkpointing.

6 Experimentation

We use experiments to verify the claims made in the Phase A/B analysis and in Section 5.2.1, along with providing a comparison to the heuristics in the current RSSP and general literature.

6.1 Different Input Distributions

To evaluate robustness beyond the uniform model used in the analysis, we run the proposed method on several i.i.d. input distributions with substantially different shapes (e.g., multimodal, heavy-tailed, and approximately Gaussian). Notably, we include Student's t -distributions with low degrees of freedom ($\nu \in \{1, 2\}$) to test extreme heavy-tailed behavior where the input variance is infinite or undefined. Across all tested distributions, the empirical error-runtime curves exhibit the same qualitative scaling behavior predicted by theory; differences are primarily in constant factors, typically within an order of magnitude. This supports the claim that the method's decay rate is largely distribution-insensitive.

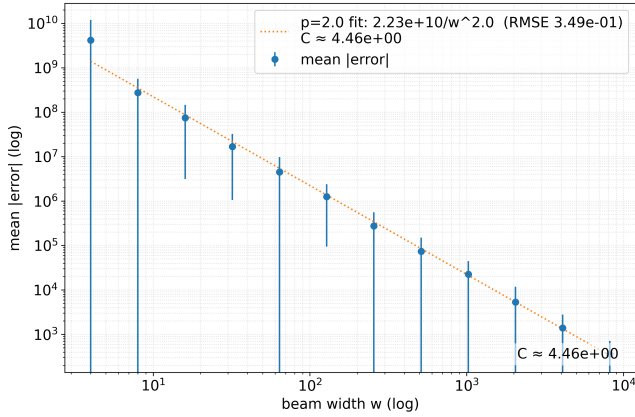


Figure 1: Performance of the proposed method on a symmetric bimodal input distribution. Error scaling remains comparable to the baseline distribution up to constant factors, indicating robustness to multimodality.

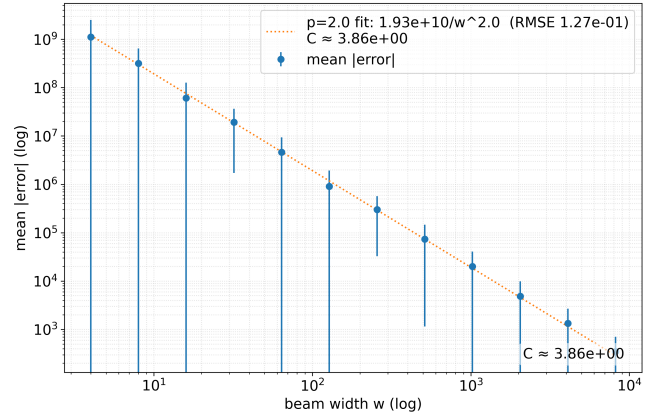


Figure 3: Performance of the proposed method on a symmetric normal input distribution. Results closely match those obtained under other distributions, suggesting weak dependence on the specific input distribution.

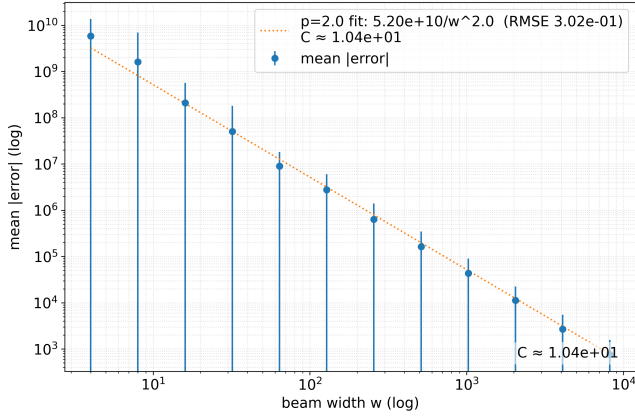


Figure 2: Performance of the proposed method on a symmetric lognormal input distribution. Despite the heavy-tailed nature of the inputs, the observed error scaling closely follows the theoretical predictions.

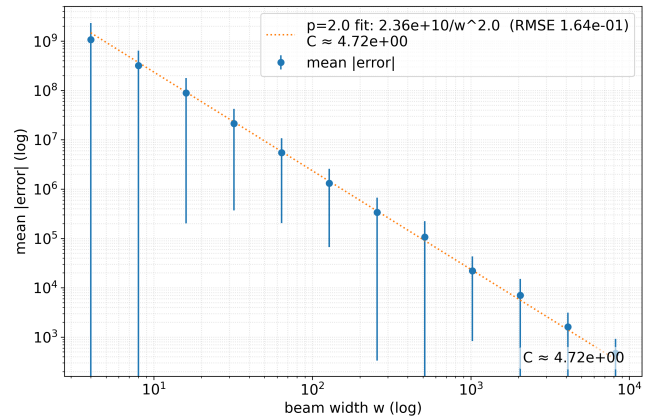


Figure 4: Performance of the proposed method on a symmetric Cauchy input distribution (Student's t with $\nu = 1$). Even with an undefined mean and variance, the inverse-quadratic decay rate is preserved.

6.2 Different Split Points

The MITM variant introduces a design choice: how many elements to allocate to Phase A (anchor construction) versus Phase B (multi-target beam refinement). The analysis predicts that allocating $O(\log w)$ elements to Phase A is sufficient to obtain an $O(B/w)$ anchor mesh while preserving enough remaining steps for Phase B to drive the inverse-quadratic decay. We validate this prediction by comparing the theoretically motivated $O(\log w)$ split against a naive halfway split and an intentionally undersized $O(1)$ split.

6.3 Dependence on n

Although not essential to the paper, we analyze the effect of the amount of elements on the performance of the algorithm. Firstly, we analyze the "medium- n " regime, where $n - n_{pre} = \Theta(n)$, but the logarithmic cost of Phase A and burn-in are not negligible. In this

case, systematic bias can be seen in the decay, as the burn-in cost becomes less significant. This is shown in Figure 10.

In the "large- n " regime, where $n \gg n_{pre}$, burn-in and Phase A cost is negligible, yielding a clean $1/n$ dependency, as shown in Figure 11.

6.4 Ablation Studies

Finally, we isolate the contributions of a key algorithmic component via an ablation; We replace the Phase A bucketing rule with a simpler equi-sampling baseline.

6.5 Tail Analysis

This section evaluates the algorithm's performance when the target value lies in the extreme tails of the subset sum distribution.

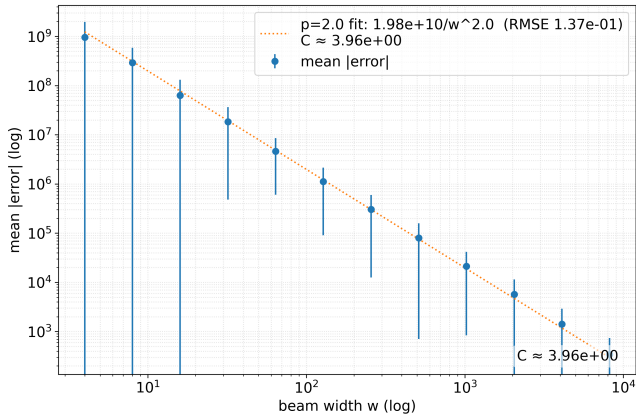


Figure 5: Performance on a symmetric Student’s t input distribution with $\nu = 2$. The infinite variance of the inputs does not break the $O(w^{-2})$ theoretical error scaling.

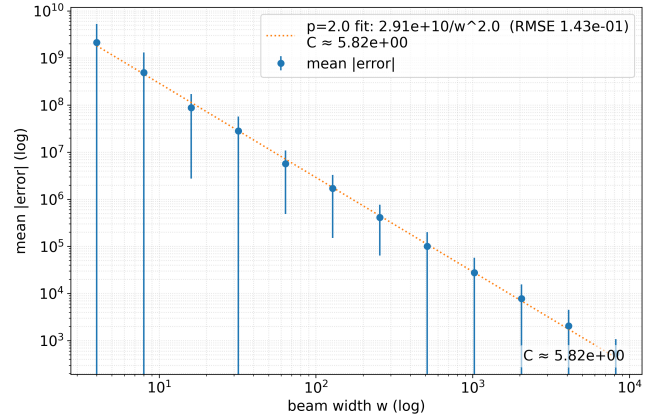


Figure 7: Effect of splitting at the theoretically motivated $O(\log w)$ point. This choice achieves the best empirical trade-off between runtime and approximation error, in line with the analytical guarantees.

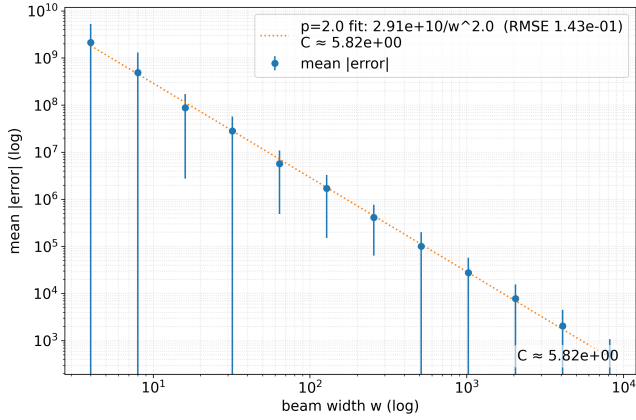


Figure 6: Performance of the proposed method on a uniform input distribution (baseline setting). Observed scaling matches the theoretical prediction up to constants.

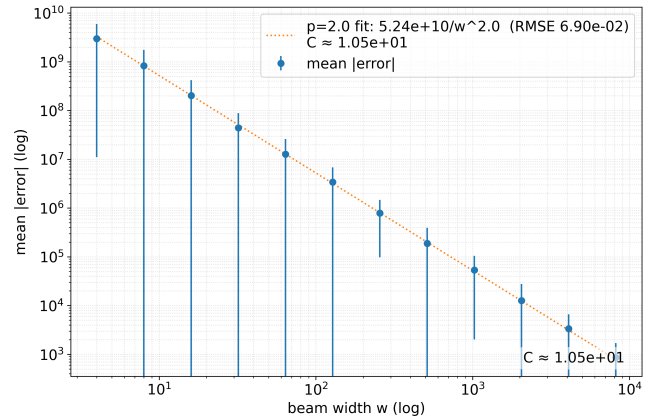


Figure 8: Effect of splitting at the halfway point. This heuristic split is competitive but typically underperforms the $O(\log w)$ split, reflecting the benefit of the theoretically guided partition.

Figure 13 illustrates the algorithmic behavior when the target is set to $T = 0.75 \sum S$ (prior to symmetrization). In this regime, the inverse-quadratic error decay rate is preserved; however, the leading constant factor degrades significantly. Furthermore, systematic drift becomes more pronounced as the beam width w increases. This drift occurs because the number of steps allocated to Phase B, defined as $n - n_{pre}$, exhibits an $O(\log w)$ dependency, which reduces the effective search depth.

Conversely, Figure 14 demonstrates the breakdown of the algorithm in an extreme tail scenario where $T = 0.95 \sum S$ (prior to symmetrization). Under these conditions, the required initial elements for the anchor phase and burn-in, n_{pre} , strictly exceed the total available elements n . The simulation’s parameterization of $n = 200$ is insufficient to absorb the $O(\log w)$ dependency inherent in n_{pre} . Consequently, Phase B is completely starved of elements,

causing the inverse-quadratic error decay guarantee to fail. This empirical breakdown is consistent with the theoretical subexponential collapse predicted for extreme targets.

6.6 Comparison Against Other Heuristics

We additionally compare our algorithm against other heuristics in the literature, including an Arithmetic Optimization Algorithm (AOA) [Madugula et al. 2022], Particle Swarm Optimization (PSO) [Kennedy and Eberhart 1995], Tabu Search (Tabu)[Glover 1989, 1990], Simulated Annealing (SA) [Kirkpatrick et al. 1983], the FPTAS by Gens and Levner [Gens and Levner 1979], and a Genetic Algorithm (GA). As shown in Figure 15, the results show that the superior error scaling of our approach allows it to quickly surpass other approaches by multiple orders of magnitude [Nguyen and Caldas 2004].

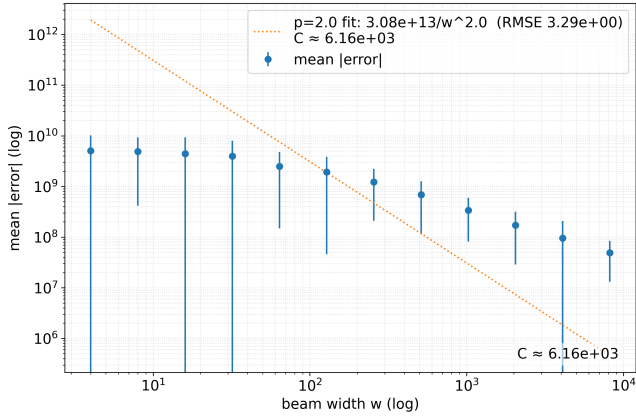


Figure 9: Failure mode when the split is too small (e.g., $O(1)$). With insufficient effort spent in Phase A, anchors are too sparse and Phase B cannot enter the multi-target small-gap regime; empirically the decay degrades to roughly inverse-linear scaling.

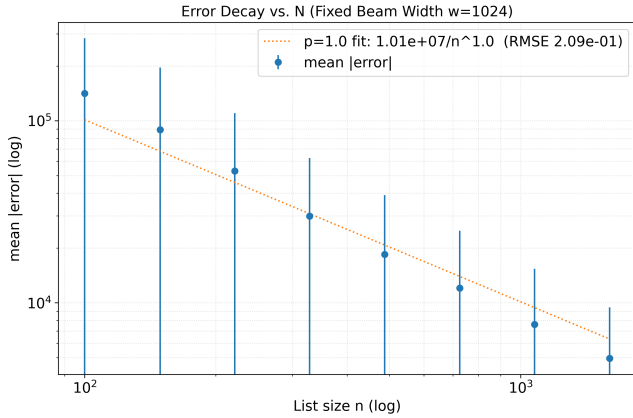


Figure 10: Effect of the number of elements (n) on empirical error scaling in the medium- n regime. Systematic bias is visible due to non-negligible Phase A and burn-in costs.

To tune each hyperparameter, Optuna with 60 outer trials (amount of hyperparameter sets to try) and 3 inner trials (amount of trials to determine hyperparameter set effectiveness) per timeframe was used. We find that this is enough to ensure convergence across all timeframes within a factor of 2, which is negligible in logspace. Detailed hyperparameter suggestions for Optuna can be found in the attached code.

In this graph specifically, standard error is used rather than standard deviation, ensuring that the graph is readable.

7 Conclusion

In this work, we transitioned the Random Subset Sum Problem (RSSP) from a strictly exact-cryptographic or worst-case perspective into a robust expected-error framework. By introducing a

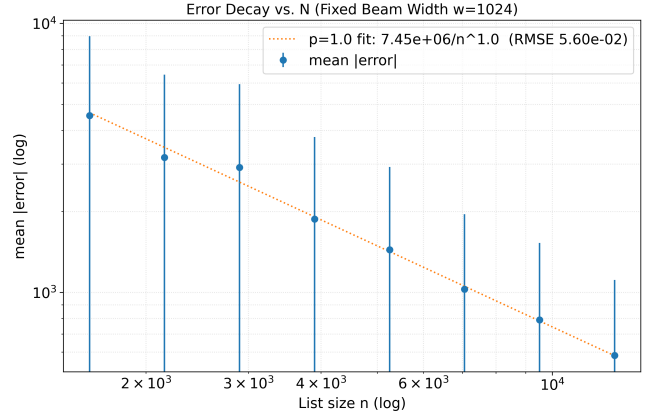


Figure 11: Effect of the number of elements (n) in the large- n regime. The decay rate exhibits a clean $1/n$ dependency as burn-in costs become negligible.

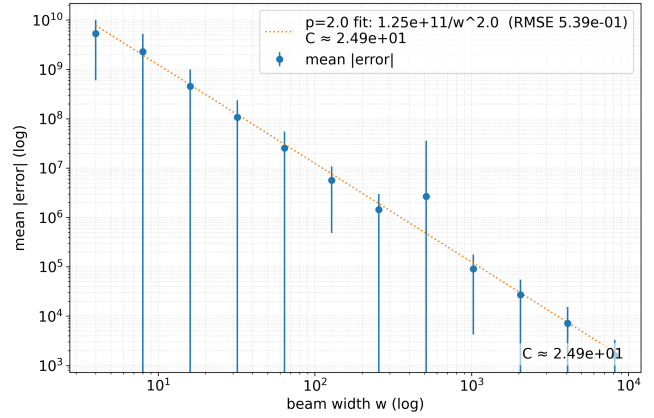


Figure 12: Ablation of Phase A sampling: replacing the proposed bucketing rule with equi-sampling. The decay rate is preserved but the constant factor increases, consistent with reduced anchor coverage quality.

Meet-In-The-Middle (MITM) beam search, we achieved a provable inverse-quadratic error decay of $\mathbb{E}|S^* - T| = \Theta(B/(nw^2))$, while maintaining a running time of $\tilde{O}(nw)$.

The theoretical foundation for this decay relies on operationalizing the mesh existence proofs of Da Cunha et al. [Da Cunha et al. 2023]. While prior work established that an $O(B/w)$ mesh exists with high probability among $O(\log w)$ random elements, our Phase A construction provides an explicit, constructive pathway to achieve this mesh without the $w^{O(C)}$ exponential state-space blowup characteristic of naive tree expansion. By applying structured bucketing and iterative trimming, we force the mesh to materialize in linearithmic time, creating a structure that Phase B can efficiently exploit. During its initial burn-in phase, Phase B relies on mechanics similar to Phase A. By modeling the Phase B iteration as an anchor convolution under a mean-field assumption, we derive

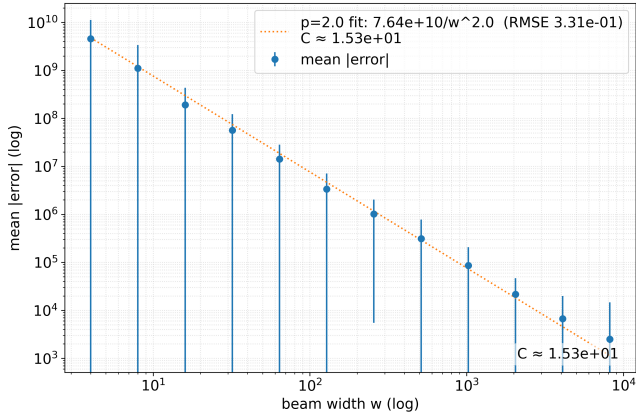


Figure 13: Performance scaling for a target moderately in the tail, $T = 0.75 \sum S$.

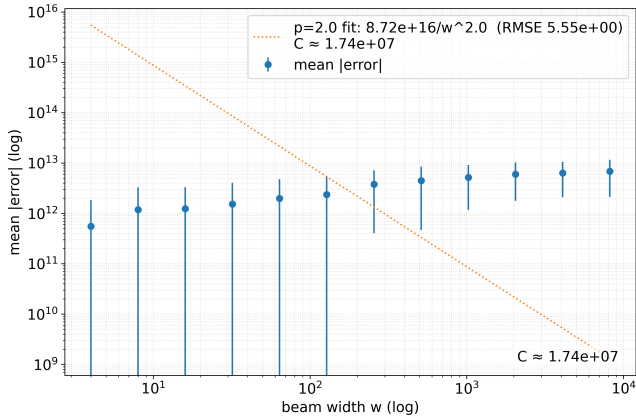


Figure 14: Failure mode for an extreme tail target, $T = 0.95 \sum S$.

a recursion that—when inverted and refined through dominance arguments—produces our stated scaling bound.

Crucially, our empirical evaluations reveal that this inverse-quadratic decay rate is remarkably robust to the underlying input distribution, extending well beyond our theoretical uniform-input assumptions. As demonstrated in Section 6, the core $O(w^{-2})$ scaling holds whether the inputs are strictly uniform, multimodal, approximately Gaussian, or even drawn from heavy-tailed Cauchy distributions with undefined variance. Furthermore, this robustness naturally extends to RSSP variants, including Vector Subset Sum and Bounded Taking Subset Sum (Appendix B). Beyond these theoretical guarantees, our framework is empirically fast, surpassing standard metaheuristics (such as AOA, PSO, and Genetic Algorithms) by multiple orders of magnitude in expected error. Together, these results position the MITM beam search as a highly practical baseline for subset sum approximation.

While this expected-error paradigm opens new avenues for studying the RSSP, important theoretical gaps remain. A primary

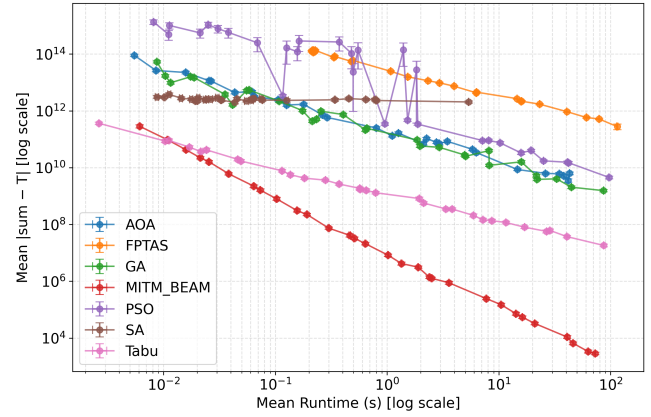


Figure 15: Approximation error versus wall-clock time for the proposed MITM beam search compared against standard heuristics: Arithmetic Optimization Algorithm (AOA), Particle Swarm Optimization (PSO), Tabu Search (Tabu), Simulated Annealing (SA), Fully Polynomial Time Approximation Scheme (FPTAS), and a Genetic Algorithm (GA). The beam-based method exhibits a markedly steeper error decay, quickly surpassing competing heuristics by several orders of magnitude in solution quality.

challenge is establishing unconditional lower bounds on the expected error for any algorithm constrained to $\tilde{O}(nw)$ time, which would formally define the limits of the small-gap regime. Finally, while we have shown that a greedy geometric decay achieves a w^{-2} bound, a compelling direction for future research is determining whether the redundant encoding and alphabet-expansion strategies used in exact representation techniques can be adapted to fundamentally accelerate this expected error decay rate.

Acknowledgments

The authors would like to thank Portland State University for the compute power required to run simulations, Tucker Mastin for valuable feedback and insight regarding evaluation, and Maxwell Chen for helping with proof validation. Claude Code was used to generate experimental harnesses used in Section 6 and Appendix B, and to generate documentation for the supplemental material.

This material is supported by the National Science Foundation under Grant Nos. 2346732, 2318139, and 2019216.

References

- Amir Abboud, Karl Bringmann, Nick Fischer, and Marvin Künnemann. 2019. AND Subset Sum is Hard: Tight Conditional Lower Bounds for Scheduling, Matching, and Related Problems. *SIAM J. Comput.* 48, 2 (2019), 539–579. doi:10.1137/16M1082018
- Anja Becker, Jean-Sébastien Coron, and Antoine Joux. 2011. Improved Generic Algorithms for Hard Knapsacks. In *Advances in Cryptology – EUROCRYPT 2011 (Lecture Notes in Computer Science, Vol. 6632)*. Springer, 364–385. doi:10.1007/978-3-642-20465-4_21
- David Biesner, Rafet Sifa, and Christian Bauckhage. 2022. Solving Subset Sum Problems using Binary Optimization with Applications in Auditing and Financial Data Analysis. *TechRxiv* – (2022), -. doi:10.36227/techrxiv.18994160.v1 Preprint.
- Xavier Bonnetain, Rémi Bricout, André Schrottenloher, and Yixin Shen. 2020. Improved Classical and Quantum Algorithms for Subset-Sum. In *Advances in Cryptology – ASIACRYPT 2020 (Lecture Notes in Computer Science, Vol. 12492)*. Springer, 633–666. doi:10.1007/978-3-030-64834-3_22

- Christian Borgs, Jennifer T Chayes, and Boris Pittel. 2001. Phase transition and finite-size scaling for the number partitioning problem. *Random Structures & Algorithms* 19, 3-4 (2001), 247–288.
- Lin Chen, Jiayi Lian, Yuchen Mao, and Guochuan Zhang. 2024a. Approximating Partition in Near-Linear Time. In *Proceedings of the 56th Annual ACM Symposium on Theory of Computing (STOC 2024)*. ACM, New York, NY, USA, 307–318. doi:10.1145/3618260.3649727
- Lin Chen, Jiayi Lian, Yuchen Mao, and Guochuan Zhang. 2024b. Faster Algorithms for Bounded Knapsack and Bounded Subset Sum Via Fine-Grained Proximity Results. In *Proceedings of the 2024 ACM–SIAM Symposium on Discrete Algorithms (SODA)*. Society for Industrial and Applied Mathematics, Philadelphia, PA, USA, 4828–4848. doi:10.1137/1.9781611977912.171
- Matthijs J. Coster, Antoine Joux, Brian A. LaMacchia, Andrew M. Odlyzko, Claus-Peter Schnorr, and Jacques Stern. 1992. Improved Low-Density Subset Sum Algorithms. *Computational Complexity* 2, 2 (1992), 111–128. doi:10.1007/BF01201999
- Arthur Carvalho Walraven Da Cunha, Francesco d’Amore, Frédéric Giroire, Hicham Lesfari, Emanuele Natale, and Laurent Viennot. 2023. Revisiting the Random Subset Sum Problem. In *31st Annual European Symposium on Algorithms (ESA 2023) (Leibniz International Proceedings in Informatics (LIPIcs), Vol. 274)*, Inge Li Gørtz, Martin Farach-Colton, Simon J. Puglisi, and Grzegorz Herman (Eds.). Schloss Dagstuhl – Leibniz-Zentrum für Informatik, Dagstuhl, Germany, 37:1–37:11. doi:10.4230/LIPIcs.ESA.2023.37
- Abraham D. Flaxman and Bartosz Przydatek. 2005. Solving Medium-Density Subset Sum Problems in Expected Polynomial Time. In *STACS 2005 (Lecture Notes in Computer Science, Vol. 3404)*, Volker Diekert and Bruno Durand (Eds.). Springer, Berlin, Heidelberg, 305–314. doi:10.1007/978-3-540-31856-9_25
- Jonathan Frankle, Gintare Karolina Dziugaite, Daniel M. Roy, and Michael Carbin. 2020. Linear Mode Connectivity and the Lottery Ticket Hypothesis. In *Proceedings of the 37th International Conference on Machine Learning (ICML)*. Proceedings of Machine Learning Research (PMLR), Virtual Event, 3259–3269. https://proceedings.mlr.press/v119/frankle20a.html
- Michael R. Garey and David S. Johnson. 1979. *Computers and Intractability: A Guide to the Theory of NP-Completeness* (1st ed.). W. H. Freeman and Company, San Francisco, CA, x, 338 pages.
- George Gens and Eugene Levner. 1979. Fast approximation algorithms for knapsack type problems. *System Modeling and Optimization* 8 (1979), 277–281. doi:10.1007/BFb0006603
- Fred Glover. 1986. Future paths for integer programming and links to artificial intelligence. *Computers & Operations Research* 13, 5 (1986), 533–549. doi:10.1016/0305-0548(86)90048-1
- Fred Glover. 1989. Tabu Search—Part I. *ORSA Journal on Computing* 1, 3 (1989), 190–206. doi:10.1287/ijoc.1.3.190
- Fred Glover. 1990. Tabu Search—Part II. *ORSA Journal on Computing* 2, 1 (1990), 4–32. doi:10.1287/ijoc.2.1.4
- David E. Goldberg. 1989. *Genetic Algorithms in Search, Optimization and Machine Learning* (1st ed.). Addison-Wesley. Addison-Wesley Professional.
- Ellis Horowitz and Sartaj Sahni. 1974. Computing Partitions with Applications to the Knapsack Problem. *J. ACM* 21, 2 (April 1974), 277–292. doi:10.1145/321812.321823
- Nick Howgrave-Graham and Antoine Joux. 2010. New Generic Algorithms for Hard Knapsacks. In *Advances in Cryptology – EUROCRYPT 2010 (Lecture Notes in Computer Science, Vol. 6110)*. Springer, 235–256. doi:10.1007/978-3-642-13190-5_12
- Liang Huang, Kai Zhao, and Mingbo Ma. 2017. When to Finish? Optimal Beam Search for Neural Text Generation (modulo beam size). In *Proceedings of the 2017 Conference on Empirical Methods in Natural Language Processing (EMNLP)*, Martha Palmer, Rebecca Hwa, and Sebastian Riedel (Eds.). Association for Computational Linguistics, Copenhagen, Denmark, 2134–2139. doi:10.18653/v1/D17-1227
- James Kennedy and Russell C. Eberhart. 1995. Particle Swarm Optimization. In *Proceedings of IEEE International Conference on Neural Networks (ICNN’95)*, Vol. 4. IEEE, 1942–1948. doi:10.1109/ICNN.1995.488968
- Scott Kirkpatrick, C. D. Gelatt Jr., and M. P. Vecchi. 1983. Optimization by Simulated Annealing. *Science* 220, 4598 (1983), 671–680. doi:10.1126/science.220.4598.671
- Jeffrey C. Lagarias and Andrew M. Odlyzko. 1985. Solving Low-Density Subset Sum Problems. *J. ACM* 32, 1 (1985), 229–246. doi:10.1145/2455.2461
- Murali Krishna Madugula, Santosh Kumar Majhi, and Nibedan Panda. 2022. An Efficient Arithmetic Optimization Algorithm for Solving Subset-sum Problem. In *2022 International Conference on Connected Systems & Intelligence (CSI)*. IEEE, Piscataway, NJ, USA, 1–7. doi:10.1109/CSI54720.2022.9923996
- Stephan Mertens. 1998. Phase transition in the number partitioning problem. *Physical Review Letters* 81, 20 (1998), 4281.
- Trung Dung Nguyen and Carlos H. Caldas. 2004. A Genetic Algorithm for the Subset Sum Problem. *Neurocomputing* 61, 1–3 (2004), 453–459. doi:10.1016/j.neucom.2003.11.025
- Richard Schroepel and Adi Shamir. 1981. A $T = O(2^{n/2})$, $S = O(2^{n/4})$ Algorithm for Certain NP-Complete Problems. *SIAM J. Comput.* 10, 3 (Aug. 1981), 456–464. doi:10.1137/0210033
- David Wagner. 2002. A generalized birthday problem. In *Annual International Cryptology Conference*. Springer, 288–303.

- Sam Wiseman and Alexander M. Rush. 2016. Sequence-to-Sequence Learning as Beam-Search Optimization. In *Proceedings of the 2016 Conference on Empirical Methods in Natural Language Processing (EMNLP)*. Association for Computational Linguistics, Austin, Texas, 1296–1306. doi:10.18653/v1/D16-1137
- Zhihui Zhou and Zongzhang Zhang. 2020. Beam Search for Optimization. In *Proceedings of the AAAI Conference on Artificial Intelligence*, Vol. 34. Association for the Advancement of Artificial Intelligence (AAAI), 6744–6751. doi:10.1609/aaai.v34i04.6162

A Variance of Error

Variance bound in the random-phase regime. Let D_t denote the global gap at Phase B step t , and define the one-step improvement $\Delta_t := D_t - D_{t+1} \geq 0$.

In the random-phase, small-gap regime $D_t \ll \Delta = B/w$ we have

$$\mathbb{E}[\Delta_t | D_t] = \Theta\left(\frac{w^2}{B}\right)D_t^2, \quad \text{Var}(\Delta_t | D_t) = \Theta\left(\frac{w^2}{B}\right)D_t^3.$$

Set $Y_t := 1/D_t$. A second-order expansion gives

$$\Delta Y_t = Y_{t+1} - Y_t = \frac{\Delta_t}{D_t^2} + \frac{\Delta_t^2}{D_t^3} + o(\Delta_t^2).$$

Drift of Y_t . Taking conditional expectations and using the above moments,

$$\mathbb{E}[\Delta Y_t | \mathcal{F}_{t-1}] = \Theta\left(\frac{w^2}{B}\right).$$

Summing over steps,

$$\mathbb{E}[Y_T] = Y_0 + \Theta\left(\frac{w^2}{B} T\right) = \Theta\left(\frac{w^2}{B} T\right).$$

Conditional variance of ΔY_t . From the expansion and $|\Delta_t| \leq D_t$,

$$\text{Var}(\Delta Y_t | \mathcal{F}_{t-1}) = O\left(\frac{\text{Var}(\Delta_t | \mathcal{F}_{t-1})}{D_t^4} + \frac{\mathbb{E}[\Delta_t^4 | \mathcal{F}_{t-1}]}{D_t^6}\right).$$

Let $p_t = \Pr(\text{improve} | D_t) = O(\frac{w^2}{B} D_t)$ and conditional on improvement, the improvement size $S_t = D_t - D_{t+1} \sim U(0, D_t)$. Then $\Delta_t = D_t - D_{t+1} = I_t S_t$, $I_t \sim \text{Bernoulli}(p_t)$. Hence, for any $m \geq 1$,

$$\mathbb{E}[\Delta_t^m | D_t] = \mathbb{E}[(I_t S_t)^m | D_t] = \mathbb{E}[I_t S_t^m | D_t] = p_t \mathbb{E}[S_t^m | D_t].$$

Taking $m = 4$ yields

$$\mathbb{E}[\Delta_t^4 | D_t] = p_t \mathbb{E}[S_t^4 | D_t] = O\left(\frac{w^2}{B}\right)D_t^5.$$

Since $\text{Var}(\Delta_t | \mathcal{F}_{t-1}) = \Theta\left(\frac{w^2}{B}\right)D_t^3$, we obtain

$$\text{Var}(\Delta Y_t | \mathcal{F}_{t-1}) = O\left(\frac{w^2}{B} \cdot \frac{1}{D_t}\right).$$

Variance of Y_T . By the martingale variance identity,

$$\text{Var}(Y_T) = \sum_{t=1}^T \mathbb{E}[\text{Var}(\Delta Y_t | \mathcal{F}_{t-1})] = O\left(\frac{w^2}{B} \sum_{t=1}^T \mathbb{E}\left[\frac{1}{D_t}\right]\right).$$

From the drift, $\mathbb{E}[1/D_t] = \mathbb{E}[Y_t] = \Theta\left(\frac{w^2}{B} t\right)$, giving

$$\text{Var}(Y_T) = O\left(\frac{w^2}{B} \sum_{t=1}^T \frac{w^2}{B} t\right) = O\left(\frac{w^4}{B^2} T^2\right).$$

Transforming back to D_T . Using the delta (or Lipschitz) bound for $g(y) = 1/y$,

$$\begin{aligned} \text{Var}(D_T) &= \text{Var}(g(Y_T)) \leq \frac{\text{Var}(Y_T)}{(\mathbb{E}[Y_T])^4} \\ &= O\left(\frac{(w^4/B^2)T^2}{(\frac{w^2}{B}T)^4}\right) = O\left(\frac{B^2}{w^4 T^2}\right). \end{aligned}$$

Conclusion. Hence in the random-phase, small-gap regime,

$$\text{Var}(D_T) = O\left(\frac{B^2}{w^4 T^2}\right).$$

B Adapting to Variants

B.1 Bounded Taking

The Bounded Taking variant of Subset Sum restricts the solution to at most k elements. Consider the canonical setting where the target is $T = 0$, inputs are drawn from $U(-B, B)$, and a valid solution must contain at least one element. In this setting, the Bernoulli symmetrization transform is natively bypassed. We can adapt the MITM beam search to accommodate the cardinality constraint k while preserving the expected error decay, provided k is sufficiently large.

B.1.1 Natural Logarithmic Sparsity and Error Decay. Introducing a strict budget k limits the maximum number of improvements the algorithm can make, as an improvement only occurs on an inclusion branch. Because the unconstrained expected error is $O(B/(nw^2))$, the algorithm requires a global distance reduction factor of roughly nw .

Surprisingly, the optimal solutions found by this framework are naturally logarithmically sparse.

LEMMA B.1 (CONCENTRATION OF STOCHASTIC ERROR DECAY). *Let $D_0 = \Theta(B/w)$ be the initial Phase B gap. To achieve a target error of $D_{\text{target}} = \Theta(B/(nw^2))$ with probability $1 - \delta$, Phase B requires a budget of only $k_B = \lceil \ln(nw) \rceil + O(\sqrt{\ln(nw) \ln(1/\delta)})$.*

PROOF. By Lemma 5.6, conditional on an improvement, the new distance D' is stochastically dominated by a uniform distribution on $[0, D]$. After m successful improvements, the error can be upper-bounded by:

$$D_m = D_0 \prod_{i=1}^m U_i, \quad U_i \stackrel{i.i.d.}{\sim} U(0, 1).$$

To find the number of steps m needed to achieve a reduction ratio of $D_0/D_m = nw$, we apply the negative natural logarithm:

$$-\ln\left(\frac{D_m}{D_0}\right) = \sum_{i=1}^m -\ln(U_i).$$

Let $X_i = -\ln(U_i)$. The standard uniform distribution transformed by $-\ln$ yields a standard exponential distribution: $X_i \sim \text{Exp}(1)$, with $\mathbb{E}[X_i] = 1$ and $\text{Var}(X_i) = 1$. The sum of m independent $\text{Exp}(1)$ variables exactly follows a Gamma distribution:

$$S_m = \sum_{i=1}^m X_i \sim \Gamma(m, 1),$$

where $\mathbb{E}[S_m] = m$ and $\text{Var}(S_m) = m$. We require $S_m \geq \ln(nw)$. Because $\mathbb{E}[S_{k_B}] = k_B$, setting $k_B \approx \ln(nw)$ achieves the target reduction in expectation. Applying standard Chernoff bounds for the Gamma distribution, padding the required budget by the standard deviation ensures concentration:

$$k_B = \lceil \ln(nw) \rceil + c\sqrt{\ln(nw) \ln(1/\delta)},$$

which guarantees $S_{k_B} \geq \ln(nw)$ with probability at least $1 - \delta$. \square

Phase A consumes at most $O(\log w)$ budget. Thus, if the global budget satisfies $k \geq \Theta(\log n + \log w)$, the cardinality constraint is essentially non-binding, since if $k < O(\log(nw))$ then the problem can be solved in subexponential time. The Bounded Taking variant will naturally converge on the full $O(B/(nw^2))$ unconstrained error decay, proving that our method creates solutions that are naturally sparse.

This provides a distinct advantage over existing approaches. Standard dynamic programming and FPTAS methods typically require an augmented state space to enforce cardinality constraints, scaling complexity by a factor of k . Furthermore, to the best of our knowledge, analyses of representation-based techniques [Howgrave-Graham and Joux 2010] and standard metaheuristics do not establish expected logarithmic sparsity bounds. Therefore, the ability of the MITM beam search to naturally converge on $O(\log(nw))$ -sparse solutions represents a novel structural guarantee for the Bounded Taking variant.

B.2 Adapting to Vector Subset Sum

The Vector Subset Sum Problem (VSSP) generalizes to d dimensions: given $\mathbf{v}_1, \dots, \mathbf{v}_n \in \mathbb{Z}^d$ with $\|\mathbf{v}_i\|_\infty \leq B$ and target $\mathbf{T} \in \mathbb{Z}^d$, minimize $\|\sum_{\mathbf{v} \in V} \mathbf{v} - \mathbf{T}\|_2$. The MITM beam search adapts with three changes: Phase A buckets become hypercube cells ($w^{1/d}$ per axis, w total, side $\Delta = B/w^{1/d}$), scoring uses Euclidean distance, and symmetrization applies coordinate-wise.

Phase A. The logistic filling dynamics carry over: each filled cell contributes $\Omega(1/w)$ filling probability per unfilled cell (via a d -dimensional checkerboard disjointness argument), so all w cells fill in $O(\log w)$ steps w.h.p., yielding mesh gap $O(B\sqrt{d}/w^{1/d})$.

Phase B. The key difference is geometric. Each (beam element, anchor) pair at distance D contributes an improvement region that is a d -ball of volume $V_d D^d$. With $\Theta(w^2)$ disjoint pairs in the small-gap regime, the improvement probability becomes $\Pr(\text{improve} \mid D) = \Theta(w^2 V_d D^d / B^d)$. Conditional on improvement, the new distance satisfies $\mathbb{E}[D'] = \frac{d}{d+1} D$ (expectation of the radial coordinate of a uniform point in a d -ball). The resulting drift is

$$\mathbb{E}[D_{t+1} - D_t \mid D_t = D] \leq -c_d \frac{w^2}{B^d} D^{d+1}.$$

Substituting $Y_t = D_t^{-d}$ gives $Y_{t+1} \geq Y_t + dk$, so $D_t = O(B/(w^2 t)^{1/d})$. Setting $t = \Theta(n)$:

THEOREM B.2 (MITM BEAM FOR VECTOR SSP). *Under the same conditions as Theorem 5.11 but in d dimensions, the MITM beam search returns \mathbf{S}^* satisfying*

$$\mathbb{E}[\|\mathbf{S}^* - \mathbf{T}\|_2] = O\left(\frac{B}{(nw^2)^{1/d}}\right),$$

in $O(nw \log w \cdot d)$ time and $O(wd)$ memory, using a KDTree as long as $n \gg 2^d$.

As illustrated in Figure 16, this is empirically consistent across $d \in \{2, 3, 5\}$. The exponent degrades from w^{-2} to $w^{-2/d}$, reflecting that d -ball volume scales as D^d , making each unit of distance reduction harder.

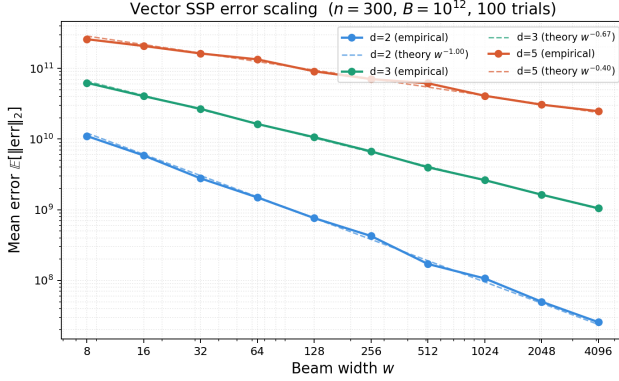


Figure 16: Empirical error scaling of the proposed MITM beam search applied to the Vector Subset Sum Problem across $d \in \{2, 3, 5\}$. Results confirm the theoretical $w^{-2/d}$ exponent degradation.

C Proofs for Phase B Burn-in

This appendix provides the formal proofs for the burn-in dynamics summarized in Lemma 5.5, specifically detailing the random walk into the target range and the monotonicity guarantees that allow Voronoi cells to fill.

Phase 1: reaching the anchor range. Without loss of generality assume all $z \in Z$ are positive. Before any beam element enters Q , the scoring rule preserves the largest beam values. Hence negative increments are never retained, and the maximum beam element evolves as

$$M_k := \sum_{t=1}^k Y_t, \quad Y_t := \max\{0, s_t\}, \quad s_t \sim U([-B, B]).$$

The variables $\{Y_t\}$ are i.i.d. with exact mean and variance: $\mathbb{E}[Y_t] = \frac{B}{4}$, and $\text{Var}(Y_t) = \frac{5B^2}{48}$. Let $m := \min Z$. By the Central Limit Theorem, $M_k \sim \mathcal{N}\left(k\frac{B}{4}, k\frac{5B^2}{48}\right)$. To ensure $M_k \geq m$ with high probability $1 - \delta$, we solve for k using the standard normal quantile $z_{1-\delta}$:

$$k\frac{B}{4} - z_{1-\delta}\sqrt{k\frac{5B^2}{48}} \geq m.$$

This yields a required step count of $k \approx \frac{4m}{B} + O\left(\sqrt{\frac{m}{B}}\right)$.

Phase 2: expansion inside Q (filling all Voronoi cells). Let $\{V_1, \dots, V_m\}$ be the Voronoi partition of the line induced by Z . Under the $\Theta(B/w)$ -spacing guarantee from Phase A, there exists an absolute constant $\alpha \in (0, 1)$ such that for all j , $\text{Leb}(V_j \cap Q) \geq \alpha \cdot \frac{B}{w}$.

Define the set of occupied Voronoi cells at time t as $\mathcal{F}_t := \{j : \exists x \in \mathcal{W}_t \cap Q \text{ with } x \in V_j\}$, and let $K_t := |\mathcal{F}_t|$.

LEMMA C.1 (ERROR MONOTONICITY). *The minimum error/distance at time t , $D(t)$, monotonically decreases.*

PROOF. Let $\text{Dist}(\mathcal{S}) = \min |\mathcal{S}_i - T|$. After an expansion $\mathcal{W}'_i = \mathcal{W}_i \cup \mathcal{W}_i + s_i$, \mathcal{W}'_i will be a superset of \mathcal{W}_i . If the scoring heuristic H satisfies $\text{Dist}(H(\mathcal{S}^{(1)})) \leq \text{Dist}(H(\mathcal{S}^{(2)}))$ where $\mathcal{S}^{(1)} \subseteq \mathcal{S}^{(2)}$, error monotonically decreases. The scoring heuristics trivially satisfy this property because preserving local minima also preserves global minima. \square

LEMMA C.2 (FILLING MONOTONICITY). *After any beam element \mathcal{W}_i enters Q , any filled Voronoi cell cannot be vacated.*

PROOF. Inside $[-\min Z, \max Z]$, having one anchor every two buckets guarantees a spacing of at most 2Δ . The condition that \mathcal{W}_i enters Q ensures it does not stray more than $c\frac{B}{w} \leq 2\Delta$. A minimum spacing of 2Δ guarantees $\mathcal{H} \neq \emptyset$. By Lemma C.1, minimum error is monotonically decreasing, hence the scoring heuristic permanently switches to OnePerBucket. A filled Voronoi cell is not subject to truncation that would vacate it. \square

LEMMA C.3 (VORONOI-CELL FILLING AFTER ENTERING Q). *Assume that at time t_0 the beam has at least one element in Q . There exists an absolute constant $c > 0$ such that for all $t \geq t_0$,*

$$\mathbb{E}[K_{t+1} - K_t \mid \mathcal{F}_t] \geq c \cdot (m - K_t) \cdot \frac{K_t}{w}.$$

Consequently,

$$\Pr\left(K_{t_0+C_1 \log w} = m\right) \geq 1 - w^{-\Omega(1)}.$$

PROOF. Fix $t \geq t_0$ and condition on \mathcal{F}_t with $K_t = K$. Pick any unoccupied cell index $j \notin \mathcal{F}_t$. For every $i \in \mathcal{F}_t$, there is $x_i \in \mathcal{W}_i \cap Q$ with $x_i \in V_i$. The event that $x_i + s_{t+1} \in V_j \cap Q$ requires $s_{t+1} \in (V_j \cap Q) - x_i$. Since $x_i \in Q$ and Q has width $\Theta(B)$, the translate intersects $[-B, B]$ with measure $\Omega(\text{Leb}(V_j \cap Q))$. There is an absolute constant $\beta > 0$ such that $\Pr(x_i + s_{t+1} \in V_j \cap Q \mid \mathcal{F}_t) \geq \beta \cdot \frac{1}{w}$.

Taking the K occupied representatives, a union bound gives $\Pr(\exists i \in \mathcal{F}_t : x_i + s_{t+1} \in V_j \cap Q \mid \mathcal{F}_t) \geq \min\{1, \beta\frac{K}{w}\}$. Summing over the $(m - K)$ unoccupied cells yields the discrete logistic growth lower bound. Standard comparison implies K_t reaches m in $O(\log w)$ additional steps. \square

D Experimental Methodology and Parameters

This appendix specifies the experimental protocol used to generate the figures in Section 6. The goal is reproducibility: the details below give a summary of benchmark implementation used to generate all plots. Code for all experiments is provided in the supplementary material.

D.1 Metric, averaging, and plots

Each method run outputs a candidate subset sum S and we report absolute error

$$\text{err} = |S - T|.$$

For each configuration (distribution, split rule, beam width), we run independent trials and aggregate the sample mean and sample standard deviation across trials. All reported scaling plots show $\mathbb{E}[\text{err}]$ with error bars of one sample standard deviation. All scaling plots are displayed on log-log axes.

D.2 Instance generation

Each trial samples n i.i.d. integers from a specified family and a target T using one of two target rules.

Distribution families. We evaluate several qualitatively different i.i.d. input families. Each family is evaluated in either a *symmetric* form (approximately supported on $[-B, B]$) or a *nonnegative* form (supported on $[0, B]$). All families are integer-valued via rounding. Specifically:

- **Uniform.** Discrete uniform sampling on $[-B, B]$ (symmetric) or $[0, B]$ (nonnegative).
- **Normal.** Gaussian with mean 0 and standard deviation $\sigma \approx B/3$, clipped to the relevant interval and rounded. The nonnegative form takes $|X|$ before clipping.
- **Lognormal.** A lognormal magnitude with moderate spread, rescaled so that typical values are comparable to B , then clipped and rounded. The symmetric form assigns a random sign.
- **Bimodal.** A two-component Gaussian mixture: in the symmetric setting the two modes are centered at approximately $\pm B/3$ with standard deviation about $B/10$; in the nonnegative setting the modes are centered near 0 and B .
- **Student's t .** A Student's t variate with ν degrees of freedom (default $\nu = 2$, giving infinite variance), scaled by $B/4$ and clipped to $[-B, B]$ after rounding. The nonnegative form takes the absolute value before clipping. Setting $\nu = 1$ yields the Cauchy distribution (infinite mean and variance).

All experiments use a fixed magnitude parameter B across distributions to keep dynamic range comparable (the benchmark uses $B = 10^{12}$ unless otherwise stated).

Target generation. Targets are generated as follows: Choose a uniformly random subset of the sampled items (each item independently included with probability $1/2$) and set T to the sum of that subset. This guarantees at least one exact solution exists.

D.3 Proposed method configuration

All experiments evaluate the meet-in-the-middle beam method described in Section 5. The item list is split into a left stage (Phase A) and a right stage (Phase B). Phase A builds a set of anchors; Phase B runs a width- w beam search scored by distance to the set of residual targets induced by the anchors.

Beam width grid. We evaluate a geometric grid of beam widths w (powers-of-two style): starting from a minimum value, repeatedly multiply by 2 up to a maximum. Unless otherwise stated, this grid matches the one used in the benchmark driver for the corresponding figure.

Split strategies. We evaluate several split rules:

- **Half split.** Split at $n/2$.
- **Fixed split.** Split at a fixed index (used to demonstrate failure when Phase A is intentionally undersized).
- **Logarithmic split.** Split at $\lfloor c \log_2 w \rfloor$ for a chosen constant c , as motivated by the Phase A analysis.

Phase A anchoring rule. Phase A expands the current anchor set by include/exclude of each left-half item, then performs a width control step that retains a structured subset of candidates. We evaluate two Phase A variants:

- **Bucketed random representative.** Partition the fixed domain $[-B/2, B/2]$ into w equal-width buckets and keep one uniformly random candidate from each non-empty bucket.
- **Deterministic equi-sampling.** Sort the unique candidates and keep w approximately evenly spaced representatives (max-spacing style).

D.4 Parameter values

Figures 1 through 15 are run with 200 trials, $n = 200$, $B = 10^{12}$, with the target chosen as a random subset, and with the split point chosen as $\lfloor 4 \log(w) \rfloor$ unless otherwise stated.

Figure 15 is run with 100 trials, $n = 300$, and $B = 10^{15}$, with the target chosen as a random subset.

Figure 16 is run with 100 trials, $n = 300$, and $B = 10^{12}$.

Detailed hyperparameter breakdowns for each figure are available in the attached code.

D.5 Fixed-exponent reference fits

To visualize agreement with the predicted inverse-quadratic decay, we overlay a fixed-exponent reference fit of the form

$$\widehat{\mathbb{E}}[\text{err}(w)] \approx \frac{c}{w^2}.$$

The constant c is estimated by least squares on the aggregated mean errors. When reporting an implied constant in the theoretical scaling $\mathbb{E}[\text{err}] \approx C \cdot B/(nw^2)$, we convert via

$$C \approx \frac{cn}{B}.$$